COMPUTATIONAL AND EXPRESSION ANALYSIS OF RNase L

Thesis submitted to
Jawaharlal Nehru University
For the award of degree of

MASTER OF PHILOSOPHY

KUMAR SANDEEP

SCHOOL OF LIFE SCIENCES
JAWAHARLAL NEHRU UNIVERISTY
NEW DELHI – 110 067
INDIA

JANUARY, 2008

SCHOOL OF LIFE SCIENCES

JAWAHARLAL NEHRU UNIVERSITY

NEW DELHI – 110 067

CERTIFICATE

This is certified that the research work embodied in this thesis entitled "COMPUTATIONAL AND EXPRESSION ANALYSIS OF RNase L" has been carried out in the School of Life Sciences, Jawaharlal Nehru University, New Delhi – 110 067. This work is original and has not been submitted so far, in part or in full, for the award of any degree or diploma of any university.

Kumar Sandeep

Kumar Sandeep
(Candidate)

Dr. Pramod C. Rath
(Supervisor)

Prof. P. K. Yadava
(Dean, School of Life Sciences)

ACKNOWLEDGEMENTS

I sincerely acknowledge my supervisor Dr. Pramod C. Rath for introducing me to the exciting field of molecular biology and providing invaluable guidance and encouragement throughout my work. I thank him for promptly providing the requisite facilities for smooth pursuance of my work.

I sincerely thank Prof. P. K. Yadava, present Dean and Prof. R. N. K. Bamezai former Dean, School of Life Sciences for providing all necessary facilities for pursuing my research work.

I am heartened to acknowledge my senior colleagues in the laboratory, Dr. Arttatrana Pal, Krishna Prakash, Ankush Gupta, Rashmi R. Mishra and Jyothi Ramanathan for their help. I thank to my labmates Deepak, Manish, Bhaskar, Jitendra, Manasa and Rajkumar for their help and marinating the cheerful and conductive atmosphere for good research. I specially thank Mr. Ankush Gupta for his guidance and help on RNase L.

I would like to specially acknowledge the M. Sc., SLS, Lab staff Mr. Panwar, Mr. Ram Kripal, Mr. Ajit and Mr. Chote Lal for their assistance during the work.

The administrative support of Mr. S. P. Singh, A.O., Meenu Madam, all SLS staff and CIF staff, Mr. B. A. Khan, Mr. S.K. Mishra and Mr. S. P. Sharma is thankfully acknowledge.

My friends Ravi, Rambabu, Manoj, Shiv Shankar, Rishikesh, Sanjay, Pankaj, Vibhor, Nishant, Prashant and Abhishek were the ultimate source of joy and happiness. Their suggestions were always useful and infused me with fresh ideas.

My parents' constant encouragement and loving brother and sister's well wishes has enabled me to reach this stage. Words fail me here since I can never thank them enough.

Kumar Sandeep

Abbreviations

µg	microgram
µl	microliter
-/-	knockout
°C	degree celsius
2-5A	2'-5'oligoadenylate
2-5OAS	2'-5'oligoadenylate synthetase
$A_{260/280}$	absorbance at 260/280 nm wavelength
aa	amino acid
AMP	adenosine monophosphate
ATP	adenosine triphosphate
BLAST	Basic Local Alignment Search Tool
bp	base pair
cDNA	complementary DNA
conc.	concentration
ddw	double distilled water
DEPC	diethylpyrocarbonate
ds	double stranded
e.g.	example
EtBr	ethidium bromide
Fig.	figure
g	gram
h	hour
i.e.	that is
kb	kilobase
kDa	kilodalton
M	molar
mg	milligram
ml	milliliters
min	minute
mM	milimolar
MMLV	Moloney Murine Leukemia Virus
mRNA	messenger RNA

NCBI	National Center for Biotechnology Information
ng	nanogram
nm	nanometer
nr (database)	Non Redundant Database
nt	nucleotide
O.D.	optical density
PBS	phosphate buffered saline
PCR	polymerase chain reaction
pg	picogram
RNase L	2'-5'A dependent endoribonuclease L
rRNA	ribosomal RNA
RT	room temperature
RT-PCR	Reverse Transcription Polymerase Chain Reaction
v/v	volume/volume
w/v	weight /volume

Contents

I. Summary

The interferon (IFN)-inducible, 2',5'-oligoadenylate (2-5A)-dependent endoribonuclease, RNase L functions for antiviral defense in mammalian cells by RNA degradation and apoptosis. It has a unique structure with a N-terminal regulatory region containing ankyrin repeats with 2-5A cofactor binding sites and a C-terminal RNA binding and cleavage domain. RNaseL is stress-responsive and has been implicated in prostate cancer.

The present study reports computational and expression analysis of RNase L. By amino acid sequence comparisons, RNaseL has been related to the E. coli *YahD, yeast Ire1P, Dictyostelium IreA*, and an algal protein as well as mouse RNase L and human RNase L have been compared. The Results suggest that mammalian RNase L might have evolved from an ankyrin repeats containing protein of prokaryotic origin and a stress-responsive ribonuclease protein of yeast or *Dictyostelium* origin. Mouse and human RNase L are highly homologous but differ with respect to the 4th ankyrin repeat.

Expression studies of RNase L mRNA and protein in different mouse tissues showed differential expression pattern.

The study suggests RNase L homologues in other organisms and indicates a broad range of functions of mammalian RNase L. Further investigation is necessary for a deeper insight into RNase L function and evolution.

II. Introduction

II.1. Interferons (IFN)

Interference to viral growth was first reported by Issacs and Lindenman (1957) in the chick chorioallantoic egg membranes pre-exposed to heat inactivated influenza virus. The secreted factor from the chorioallantoic membranes responsible for interference with virus (inhibition) was named as "interferon" (IFN). Atanasiu and Chany (1960) demonstrated that pre-treatment of hamsters with IFN preparations prior to inoculation of polyoma virus delayed appearance of the tumors. Paucker et al. (1962) argued that murine IFN inhibited cell growth and the activity was independent of its antiviral action; Gresser et al. (1969) demonstrated that treatment of IFN could inhibit tumor growth in animals. These properties of IFNs were later proved by recombinant IFNs in 1980s and later.

Today, the interferons are well known cytokines with antiviral, antiproliferative and immunomodulatory effects; they are used as biological response modifiers for oncology, show effectiveness against multiple sclerosis. IFNs explained unique cell signaling pathway (JAK-STAT pathway), gene expression, innate and acquired immunity, action of IFN-induced genes, their drug development potential in targeting IFN production through activation of Toll like receptors (TLRs) (Borden et al, 2007).

II.1.1. Types of Interferons

The classification of the IFN family of proteins is based mainly on their sequence, chromosomal location and receptor specificity (Chelbi-Alix, 2007). There are three types of interferons known so far.

II.1.1.1. Type I IFN

The type I IFNs consist of IFN-α, -β, -ω, -ε, -κ, -δ, -τ and -ζ (limitin) (Pestka et al, 2004). Some of these like IFN-δ, -τ and -ζ are only detected in pigs/cattle, ruminants and mice respectively. All these members are induced in

virally infected cells to induce antiviral state in the uninfected cells. Most of the studies on interferons have focused mainly on IFN-α/β. IFN-α/β also shows a variety of important immunomodulatory roles in the innate immune response and also in the adaptive immune response. Additionally, a direct or indirect tumor suppression is one of the major therapeutic activities of IFN-α/β. All of the members transmit signals through a receptor complex composed of two subunits, IFNAR-1 and IFNAR-2 (Takaoka et al, 2006).

II.1.1.2. Type II and III IFN

Type II IFN comprises of IFN-γ. This cytokine is strongly produced by activated macrophages, T cells and NK cells. IFN-γ signaling is essential for the activation of macrophages to constitute the effective form of innate immunity to intracellular microorganisms, and also contributes to the development of CD4+ Th1 cells and cytotoxic CD8+ T cells (Ikeda et al., 2002). IFN-γ signals through a pair of receptor subunits, IFNGR-1 and IFNGR-2. The type III IFN consists of IFN-λs or IL-28/29. In humans, this group includes three homologous proteins, IFN-λ1-3 (IL-28A, IL-28B and IL-29). Similar to type I IFNs, they are induced upon viral infection for their antiviral activity by inducing IFN-stimulated genes e.g., OAS (2′,5′-oligoadenylate synthetase), PKR (protein kinase R, double stranded RNA-dependent) and MxA, through activation of Jak kinase(s), signal transduction and activator of transcription (STAT) factors and subsequent formation of the IFN-stimulated (ISGF) complex (Vilcek, 2003). However, the major differences are that they are structurally distinct from type I IFNs and they utilize their specific receptor subunit, IFN-λR1 or IL-28Rα, together with IL-10R2 is known to be a shared receptor subunit among IL-10, IL-22 and IL-26. In this regard, they might be separated into the third group (type III IFNs). Downstream signaling pathways activated by IFN-λs remain to be understood in further details (Takaoka et al 2006).

II.1.2. Antiviral function of Interferons

The hallmark of antiviral responses is the production of type I interferons (IFNs). Studies on mice and human cells lacking the signal transducer and activator of transcription 1 (STAT1), a signaling molecule common to all IFN receptors, have revealed that responsiveness to IFNs is absolutely critical for antiviral resistance (Dupuis et al., 2003). This is because a major function of IFNs is to increase the expression of the protein kinase (PKR), 2'-5' Oligoadenylate synthetases (OAS), adenosine deaminase acting on RNA (ADAR1), Mx, apolipoprotein B mRNA-editing enzyme catalytic polypeptide like editing complex (APOBEC), Fv, and tripartite motif (TRIM) proteins (Samuel, 2001). Among the IFN-induced proteins believed to affect virus multiplication are PKR, which inhibits translation initiation through phosphorylation of the protein synthesis initiation factor eIF-2α; the OAS synthetase family and RNase L, which mediates RNA degradation; the family of Mx protein GTPases, which appear to target viral nucleocapsids and inhibit RNA synthesis; and ADAR, which edits double-stranded RNA by deamination of adenosine to inosine.

II.2. 2-5A pathway

The 2-5A pathway is composed of at least three types of enzymatic activities, 2-5A synthetase, 2-5A-degrading enzymes, and RNase L (Fig. 1). The dsRNA, produced by virus infection, binds and activates 2-5A synthetases. The activated 2-5A synthetases convert ATP to a series of short 2',5'-linked oligoadenylates collectively referred to as 2-5A and PPi (Cayley, Davies et al., 1984). In humans, there are four related genes (OAS1, OAS2, OAS3, and OASL) encoding eight or more isoforms of 2-5A synthetase as a result of alternative splicing. To date, the only well established biochemical function of 2-5A is to activate RNase L. 2-5A binds RNase L with high affinity, converts it from an inactive, monomeric state to a potent, dimeric endonuclease (Dong and Silverman, 1995). The 2-5A must have at least one (in human) or two (in mice) 5'-phosphoryl groups and a minimum of three adenylyl residues in 2', 5' linkage (Cayley, Davies et al., 1984). Upon

activation, RNase L cleaves viral and cellular rRNAs/mRNAs at 3' of UU and UA sequences leading to the inhibition of protein synthesis. RNase L thus cleaves viral mRNAs and induce host cell apoptosis (Dong and Silverman 1995; Dong and Silverman, 1997).

II.3. Significance of present study

In addition to the antiviral, pro-apoptotic and tumor suppressor activities of RNase L, it has been implicated in a broad range of functions, e.g., stress response, translational regulation and RNA metabolism in mitochondria. RNase L is also involved in regulation of immune response(s), cell differentiation, and in certain disease-like conditions, e.g., chronic fatigue syndrome and inflammation. Recent research indicates that RNase L may posses a broad range of protein-protein interaction activities and biochemical properties under cellular conditions. This may be supported by the ankyrin repeats, protein kinase homology region and cysteine rich region in the RNase L, which are not completely understood in terms of their cellular functions and intermolecular interactions. In the present study, the computational and expression analysis of the RNase L molecule is undertaken to look for its possible broad range function(s) and its evolutionary relatedness/origin.

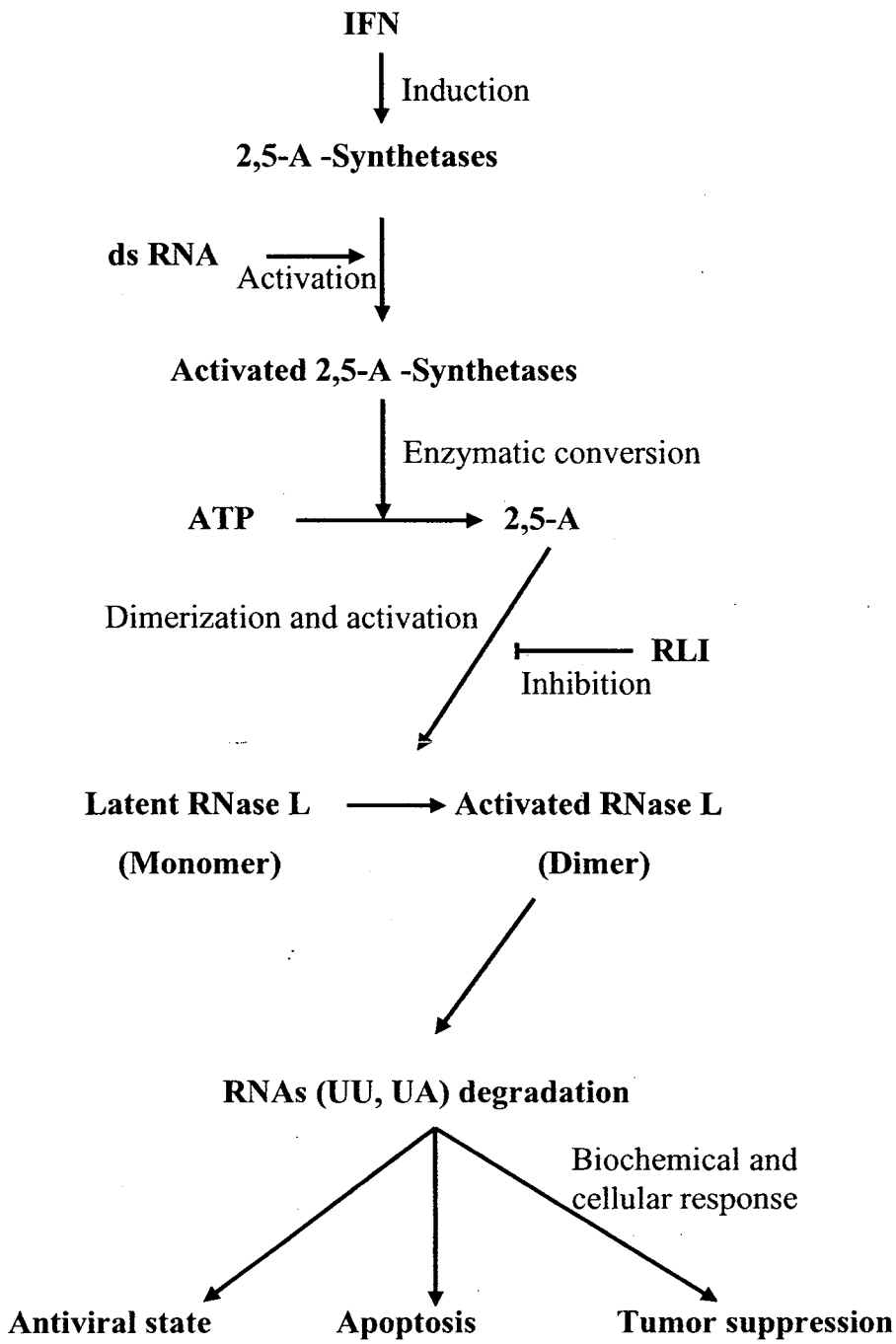

Fig.1 The 2,5-A/RNase L pathway. Both type I and II IFNs induce 2-5OAS, which synthesizes 2-5A cofactor from ATP. 2-5A activates RNase L to degrade both viral and cellular RNAs by cleavage at 3' of UU and UA sequences in the RNAs. RLI inhibits activation of RNase L by 2-5A. RNA degradation by RNase L leads to antiviral state, apoptosis and tumor supression in mammalian cells and tissues (Bisbal and Silverman, 2007).

III. REVIEW OF LITERATURE

Virus infection or interferon treatment of mammalian cells induce at least three major biochemichal pathways, which play important roles in the antiviral effects of the interferons. They are the protein kinase R (PKR) pathway, the 2-5A pathway and the MX pathway. The 2-5A pathway is constituted by 2-5A synthetases, (2-5OAS), 2-5A cofactor and the RNase L. The 2-5A cofactor activates RNase L to degrade RNAs. The 2-5OAS synthesizes the 2-5A from ATP. Virus, dsRNA, interferons induce and activate 2-5OAS, 2-5A and RNase L for the antiviral defence. Discovery of 2-5A (Kerr and Brown, 1978) as low molecular weight inhibitor of protein synthesis, on incubation of the cytoplasmic extracts from interferon-treated cells with dsRNA and ATP, led to the curiosity about the role of this small unusual oligonucleotides. The 2-5A was later shown to induce a nuclease activity (Hovanessian et al, 1979). The specificity of the 2-5A dependent endoribonuclease to UA and UU sequences was shown later (Wreschner et al, 1981). Two years later, it was shown that Interferon treatment of mouse JLS-V9R cells resulted in a 10- to 20-fold increase in the levels of the 2-5A (ppp(A2'p)nA)-dependent RNase. The nuclease was monitored in cell extracts by covalent and non-covalent binding of ^{32}P-labeled 2-5A derivatives to the nuclease and by the appearance of 2-5A-mediated ribosomal RNA cleavage products. The 2-5A dependent RNase was purified (Silverman et al, 1988) by affinity labeling of the proteins with a ^{32}P-labeled 2-5A derivative, which revealed that, the mouse 2-5A dependent RNase is a 80kDa protein.

III.1. Cloning of RNase L

Zhou et al in 1993 cloned RNase L cDNA where they used murine L929 cells and enhanced the mRNA level by treating with cycloheximide and interferon. The cDNA library was screened by bromine substituted ^{32}P-labeled 2-5A analogue (2-5A probe). A single plaque ZB1 was selected from 3 X 10^6 plaques and the protein was expressed from the clone by *in vitro* translation. The plaque showed the reactivity to both 2-5A and highly purified polyclonal antibody. Migration of the translational product in wheat germ extract showed

an apparent molecular weight of 74kDa as opposed to 80kDa purified previously. Further analysis showed that ZB1 was a partial cDNA clone encoding 74kDa polypeptide made up of 656 amino acid residues (Zhou et al, 1993).

The ZB1 was then used to screen various human libraries containing genomic DNA as well as cDNA clones, to obtain a composite human RNase L cDNA clone. The screening resulted in the partial cDNA HZB1 from human kidney cDNA library in λgt11, which was used to pick an overlapping clone HZB22. The HZB22 was then used as a probe to screen a human placenta cosmid library in the vector pWZC5 to pick the 5'-region of the coding sequence in a Sac 1-fragment. Fusion of the Sac1-fragment upstream of the Nco 1 site in ZC1 produced the clone ZC3. The coding sequences along with some flanking sequences was then subcloned into pBluescript KSII(+), resulting in the clone pZC5, whose predicted amino acid sequence resulted in an ORF encoding a polypeptide of 741 residues (83,539 Daltons) representing the human RNase L.

III.2. Biochemical properties of RNase L

RNase L is an IFN-inducible endoribonuclease for single stranded RNA.
Its general biochemical properties are:

S. No.	Property	Comments
1	Size	83.5kDa, 741aa (human) 80kDa, 735aa (mouse)
2	Functional definition	single stranded RNA binding endoribonuclease activated by 2-5A
3	Specificity	cleaves 3'- of UU, UA sequences, shows substrate specificity for ISG43 and ISG15 mRNA
4	Divalent ion effect	Mg^{++} and Mn^{++} ions enhance 2-5A binding and ribonuclease activity
5	ATP effect	ATP moderately enhances RNase L activity

III.3. Structure of RNase L

RNase L has a bipartite structure with a N-terminal regulatory domain and a C-terminal functional domain (Dong and Silverman, 1997). The structural motifs are as follows and have been diagrametically represented in Fig 2.

III.3.1. Ankyrin repeats

The ankyrin repeat was first identified in the yeast cell cycle regulator, Swi6/Cdc10 and the *Drosophila* signaling protein, Notch (Breeden and Nasmyth, 1987), and was eventually named for the cytoskeletal protein ankyrin, which contains 24 copies of this repeat (Lux et al, 1990). Ankyrin repeat containg proteins are present in all three superkingdoms including bacteria, archaea, and eukarya, as well as in a number of viral genomes. However, a phylogenetic breakdown of the organisms that contain ankyrin repeats indicates that the majority are found in eukaryotes. Modular protein domains, such as the ankyrin repeat, that act as a scaffold for molecular interactions are likely to be important for development of numerous signaling pathways necessary to evolve a more complicated multicellular organism (Marcotte et al, 1999).

The primary structure analysis of RNase L suggested that RNase L had nine ankyrin repeats, but the ninth ankyrin repeat is incomplete (Hassel et al, 1993). However, this prediction for RNase L differs from the crystal structure of ANK (Tanaka et al, 2004), which consists of eight ankyrin repeats (R1–R8). Residues 306-333, corresponding to the incomplete ninth repeat (Hassel et al, 1993) are disordered. As in other ankyrin repeat proteins (Sedwick and Smerdon, 1999), each repeat is formed by 33 amino-acid residues and consists of pairs of antiparallel α-helices stacked side by side and are connected by a series of intervening β-hairpin motifs. In general, the structure is shaped similar to a cupped hand (Jacobs and Harrison, 1998). There is a noticeable curvature across the 'palm', such that the surface created by the β-hairpins (fingers) and the α1 'inner' helices is concave, whereas that formed by the α2 'outer' helices, that is, the back of the cupped hand, is convex . The 2-5A

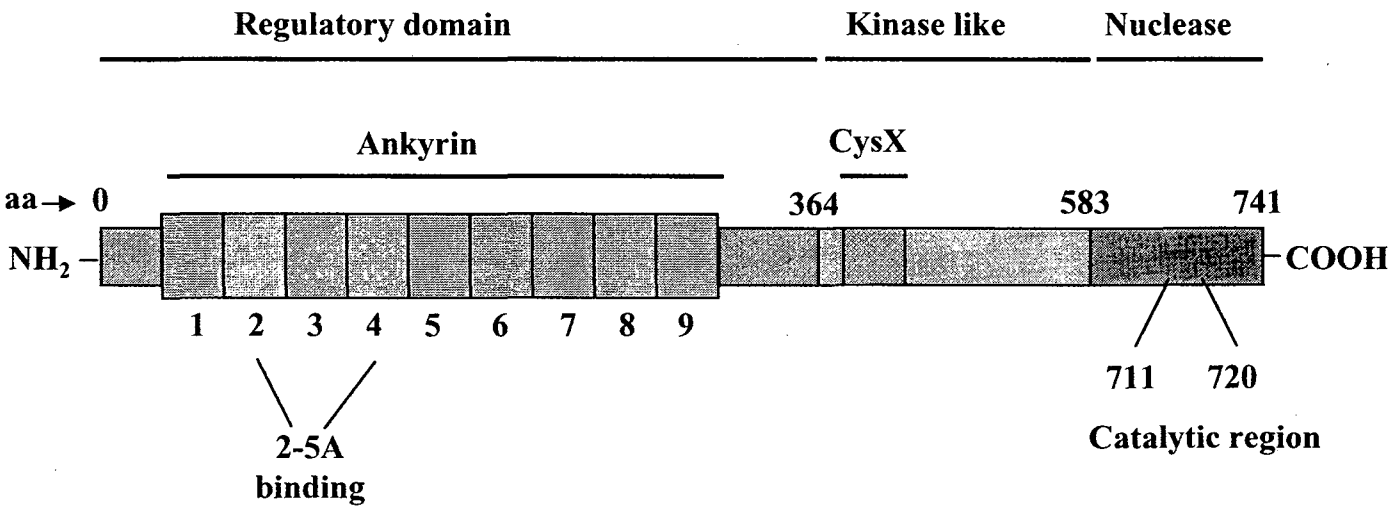

Fig.2. Bipartite structure of RNaseL. The N-terminal regulatory domain with ankyrin repeats, the protein kinase homology region with the cysteine rich sequence and the C-terminal RNA binding ribonuclease domain (711-720 aa residues form the catalytic region) are indicated. The 2-5 A cofactor binding sites are in the ankyrin repeat 2 and 4. (Bisbal et al. 2007).

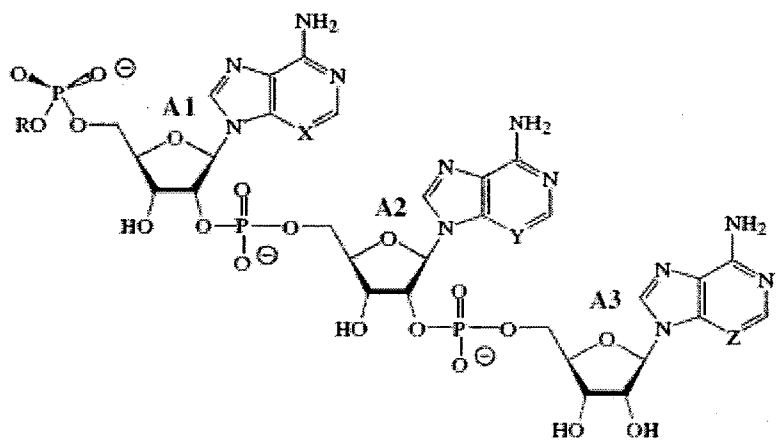

Fig.3. Structure of 2-5A (Kalinichenko et al, 2004)

molecule fits in the concavity and directly interacts with ankyrin repeats 2 and 4. The N-terminal ankyrin repeats serve as the regulatory domain of RNase L, since 2-5A binds to the ankyrin repeats 2 and 4 and activates RNase L.

III.3.2. P- loop motif (GKT motif)

Phosphate binding loop (P-loop) motifs are commonly found in many adenine and guanine binding proteins in which conserved lysine residues interact with phosphate groups of the nucleotides (Saraste et al, 1990). Presence of duplicated P-loop motif from residues 229-241 (GX_6GX_2GKT) and 253-275 [$GX9(G/X)X_9GKT$] in RNase L led to the postulation that the two GKT motifs, Gly239–Lys240–Thr241 in ankyrin 7 and Gly273–Lys274–Thr275 in ankyrin 8 are the 2-5A binding motifs (Zhou et al, 1993; Diaz-Guerra et al, 1999). Moreover substitution of the two lysines (Lys240 and Lys274) with asparagines greatly reduced the affinity for 2-5A (Zhou et al, 1993). Similarly, one mutant [NDN/CDR7-9C(24–237] (Dong and Silverman, 1997), which is truncated at both termini and lacks ankyrin 7–9, with which Lys240 and Lys274 are involved, was shown to lose 2-5A binding activity. These observations, together with the lack of structural information about ANK at the time the observations were made, led to the assumption that the two GKT motifs are the 2-5A binding motifs. However, crystal structure reported by Tanaka et al (2004) clearly revealed that the side chains of Lys240 and Lys274 are involved in an intrarepeat salt bridge with the side chains of Glu248 and Glu282, respectively, rather than in 2-5A binding. These salt bridges in ankyrin 7 and ankyrin 8 probably contribute to maintaining the folding of the ankyrin repeat domain, hence its integrity. Consequently, structural perturbation at ankyrin7 and ankyrin8 greatly diminishes the 2-5A binding ability of RNase L, even though these regions are not directly involved in 2-5A binding. This indicates conformational requirement of the ankyrin repeats for 2-5A binding and activation.

III.3.3. 2-5 A binding

Tanaka et al, (2004) crystallized 1–333 amino acids of the N-terminal ankyrin repeat domain of human RNase L with 5'-O-monophosphoryladenylyl(2'-5')adenylyl(2'-5')adenosine (p5'(A2'p5')$_2$A), a 2-5A trimer with 5'-monophosphate (Fig. 3). The crystal structure showed that the first AMP moiety of the 2-5A directly interacts with the fourth repeat of ANK. The 5'-phosphate group of the first AMP (phosphate1) forms bifurcated salt bridge with the side chain of Arg155. The side chain of Arg155 is fixed by bifurcated salt bridge with the side chain of Asp174. The adenine ring of the first AMP (adenine1) is stacked between the side chain of Phe126 and the adenine ring of the second AMP (adenine2), and is fixed by bifurcated hydrogen bonds with the side chain of Glu131, that is, OE1(Glu131)—N6(Adenine1) and OE2(Glu131)—N1(Adenine1). The side chain of Phe126 also stacks with the guanidine group of the side chain of Arg155, forming a quadruplex (Arg155–Phe126–Adenine1–Adenine2) of stacking interactions.

The second AMP moiety of 2-5A interacts only slightly with ANK. The 5'-phosphate group of the second AMP (phosphate2) is exposed to solvent, and no direct interactions are found between phosphate2 and the surface of ANK. The adenine ring of the second AMP (adenine2) is stacked with adenine1 as described above, and is fixed by a single hydrogen bond with the side chain of Tyr135, that is, OH(Tyr135)— N1(adenine2). The 3'-OH group of the second AMP is involved in a hydrogen bond network and is fixed on the protein surface via water molecules. The second AMP appears to be rather weakly fixed on the ANK surface relative to the two ends of the 2-5A molecule.

The third AMP moiety of 2-5A directly interacts with the second repeat (R2) of ANK. The 5'-phosphate group of the third AMP (phosphate3) forms a salt bridge with the side chain of Lys89. The adenine ring of the third AMP (adenine3) is stacked with the side chain of Trp60, and is fixed by a hydrogen bond network involving the side chains of Gln68 [OE1(Gln68)—N6(Adenine3) and NE2(Gln68)—N1(Adenine3)] and Asn65 [OD1(Asn65)—N6(Adenine3)], as well as a water molecule [O(Water)—N7(Adenine3)] and [O(Water)— ND2(Asn65)]. The side chain of Trp60 also stacks with the CD–

CE–NZ bonds of the side chain of Lys89, forming a triplex (Lys89–Trp60–Adenine3) of stacking interactions.

Interestingly, the 2-5A binding residues in the R4 and R2 of ANK are located at the structurally equivalent positions of the ankyrin repeats and these residues play a functionally equivalent role. The side chains of Arg155 in R4 and Lys89 in R2 form salt bridges with phosphate1 and phosphate3, respectively. The side chains of Phe126 in R4 and Trp60 in R2 stack with Adenine1 and Adenine3, respectively. Furthermore, a quadruplex (Arg155–Phe126– Adenine1–Adenine2) and a triplex (Lys89–Trp60–Adenine3) of stacking interactions are observed at R4 and R2, respectively. The side chains of Glu131 in R4 and Asn65 in R2 form hydrogen bonds with Adenine1 and Adenine3, respectively.

Based on the structure given by Tanaka et al., (2004), Nakanishi et al., (2005) used structure-based site-directed mutagenesis to identify the residues of human RNase L crucial for the recognition and binding of 2–5A. Substitution for either Trp60 or Phe126 significantly hampered the 2–5A binding ability of RNase L, as well as inactivating 2–5A-dependent RNase activity, indicating that the π-π stacking interactions of Trp60-Adenine3 and Phe126-Adenine1 are critical for 2–5A binding. Mutations of the residues Lys89 and Arg155 also led to inactivation of RNase L, indicating the importance of electrostatic interactions between Lys89-Phos3 and Arg155-Phos1 for 2–5A binding.

III.3.4. Protein kinase homology domain

RNase L bears significant homology to protein kinase domain VI and VII and some additional protein kinases in its C-terminal region. One of the opinions about the ribonuclease is that the ribonuclease evolved in part from a protein kinase which somehow lost its kinase function during evolution (Dong and Silverman, 1999). The proposed kinase domains of RNase L are either incomplete or they differ substantially from the domains of protein kinases. Domain 1 bears little similarity to the canonical protein kinase domain 1 sequence (hGXGXXGXVh, Where h is any hydrophobic residue) and in motif VII, an aspartate residue is replaced by a conserved glycine residue, in motif

VIII, a glutamine replaces an invariant glutmate, in motif IX and a conserved arginine is present in human RNase L but not in murine RNase L.

In protein kinases, a conserved lysine residue in the domain II serves to bind the α- and β-phosphoryl groups of ATP, whereas the conserved aspartate residue in domain VII serves to chelate Mg^{+} complexed with ATP. In RNase L, both of these residues are present. In fact in presence of ATP, there is enhanced RNase L activity (Wreschner et al, 1982; Krause et al, 1986). Despite the homology, however, no protein kinase activity has been detected during activation and RNA-cleavage reactions with human RNase L (Dong and Silverman, 1999). Similarly, the kinase plus ribonuclease domain of RNase L produces no detectable protein kinase activity in contrast to the phosphorylation obtained with homologous domain of the related kinase and endoribonuclease, i.e., the yeast Ire1p. In addition, neither ATP nor pA(2'p5'A)3 is hydrolyzed by RNase L. To further investigate the function of the kinase homology in RNase L, the conserved lysine residue at 392 in the protein kinase-like domain II was replaced with an arginine residue, the resulting mutant, RNase L K392R, showed >100-fold decrease in 2-5A-dependent ribonuclease activity without reducing 2-5A- or RNA-binding activities (Dong and Silverman, 1999). The greatly reduced activity of RNase LK392R was correlated to a defect in the ability of RNase L to dimerize.

Within the protein kinase region of RNase L is present a high cysteine content region (Zhou et al., 1993). The spacing of these cysteine residues ($CX_4CX_3CX_{17}CX_3C$, residues 401-436 in human RNase L) bears resemblance to some Zinc fingers, protein/nucleic acid binding domains (Dong et al, 1994). Interestingly, an argnine to glutamine mutation at 462 position in the protein kinase homology domain has been shown to be associated with prostate cancer risk or aggressiveness (Casey et al, 2002). To determine the effect of this mutations on the enzyme activity, the wild-type and mutant RNase L were compared after expression in mouse JM03 cells, isolated from a spontaneous rhabdomyosarcoma from RNase $L^{-/-}$, $p53^{-/-}$ double gene-knockout mice. The R462Q variant showed approximately one-third of the wild-type RNase L activity (Xiang et al, 2003). The deficiency in RNase L R462Q activity was correlated with a reduction in its ability to dimerize into a catalytically active form. Furthermore, RNase L R462Q was deficient in causing apoptosis in

response to 2–5A which was consistent with its possible role in the prostate cancer development.

III.3.5. RNase domain

With the cloning of partial murine clone pZB1, which lacked 89 amino acids from the C-terminal as well as RNase activity, it was clear that the RNase activity resides in the C-terminus of the molecule (Zhou et al, 1993). In 1997, Silverman and coworkers (Dong and Silverman, 1997) constructed a series of truncated RNase L proteins and found that the C-terminal 31 residues of RNase L are critical for the catalytic function of the enzyme. RNase L CΔ31, lacking residues 711–741, showed neither ribonuclease nor substrate binding activities. In contrast, RNase L CΔ21 (1-720) had full activity in presence of 2-5A. These findings clearly showed that the residues 711–720, EYRKHFPQTH, are essential for the RNA binding and ribonuclease activity of the enzyme. Later in 2001, the same group (Dong et al, 2001) mutated the amino acid residues found conserved in RNase L and *Ire1* superfamily. They found that the RNase L mutants W632A, D661A, R667A and H672A lacked ribonuclease activity. To dissect the function of the residues 711–720, EYRKHFPQTH, Nakanishi and coworkers preformed scanning mutagenesis over the 10 residues of glutathione S-transferase (GST)-fusion RNase L (Nakanishi et al, 2004). Among the single amino acid mutants examined, Y712A and F716A resulted in a significant decrease of RNase activity with a reduced RNA binding acitivity. The loss of the RNase activity was not restored by its conservative mutation, whereas the RNA binding activity was enhanced in case of Y712F. These results indicated that both Tyr712 and Phe716 provide the enzyme with a RNA binding activity and catalytic environment.

III.4. Functions of RNase L

RNase L is a multifunctional protein playing role in many important biological processes. Its functions are described below and are diagrammatically represented in Fig. 4

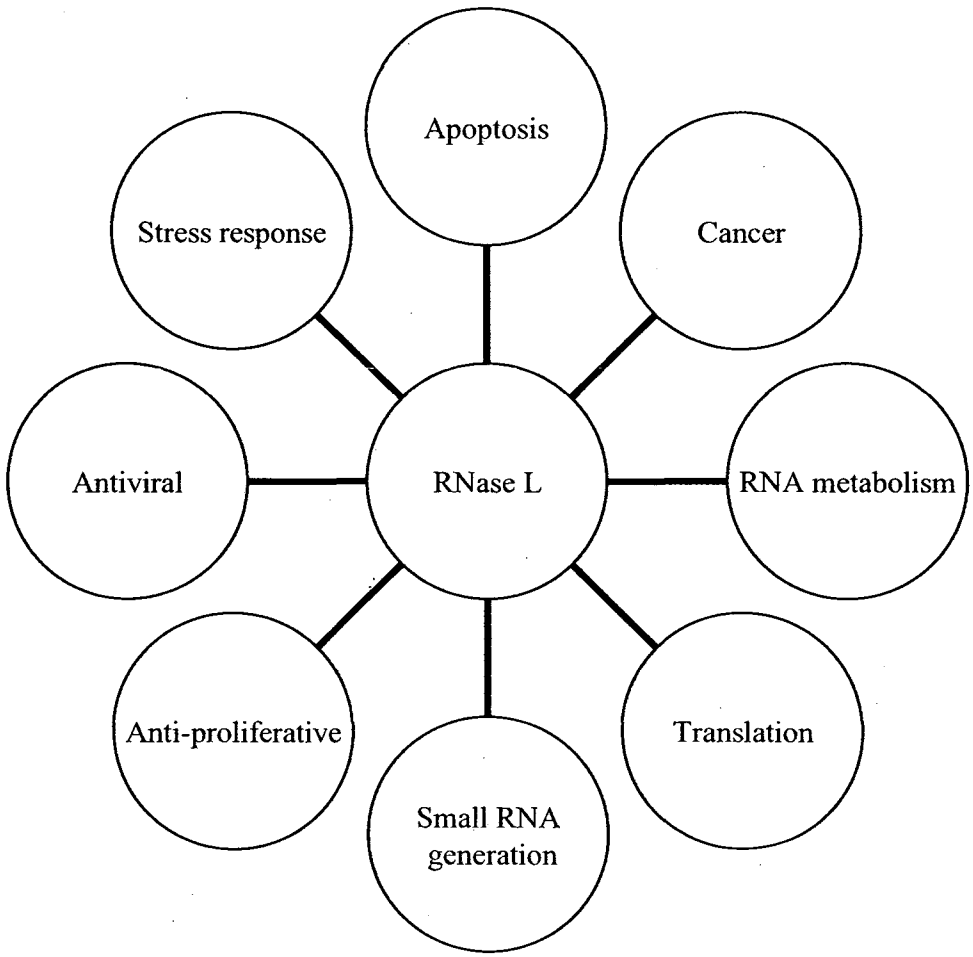

Fig.4. Multiple Functions of RNaseL. The 2-5A-dependant RNase L for antiviral defence (Samual et al, 2006), stress response (Pandey and Rath, 2004), apoptosis (Li et al, 2004), supression of cancer (Liu et al, 2007), RNA metabolism in mitocondria (Bisbal et al, 2000), regulation of translation through eRF3 (LeRoy et al, 2005), generation of small RNA for IFN-response (Malathi et al, 2007) and antiproliferation () in mammalian cells.

III.4.1 RNA metabolism

The initial studies carried out to find the sequence preferences of RNase L using poly(rC), poly(rU), poly(rA), and poly(rG) as the substrates, showed that it preferentially cleaves only poly(U) (Floyd-Smith et al, 1981, Wreschner et al, 1981). The same group showed that the activated RNase L cleaved single stranded RNA after atleast three dinucleotides (UU, UA and UG) out of 16 possible combinations. In 1994, Dong and coworkers (Dong et al, 1994) expressed RNase L in insect cells and purified the protein through fast protein chromatography. Studies with purified protein revealed sequence specificity for poly (rU) on addition of 2-5A. In contrast, poly(rA), poly(rC), poly(rG), ssDNA, dsDNA were not cleaved by RNase L.

The mechanism of RNase L-mediated antiviral activity was investigated (Li et al, 1998) following encephalomyocarditis virus (EMCV) infection of cell lines in which expression of transfected RNase L was induced or endogenous RNase L activity was inhibited. RNase L induction markedly enhanced the anti-EMCV activity of IFN via a reduction in EMCV RNA. Inhibition of endogenous RNase L activity inhibited this reduction in viral RNA. RNase L induction reduced the rate of EMCV RNA synthesis, suggesting that RNase L may target viral RNAs involved in replication early in the virus life cycle. The RNase L-mediated reduction in viral RNA occurred in the absence of detectable effects on specific cellular mRNAs and without any global alteration in the cellular RNA profile. Extensive rRNA cleavage, indicative of high levels of 2-5A, was not observed in RNase L-induced, EMCV-infected cells; however, transfection of 2-5A into cells resulted in widespread degradation of cellular RNAs. These findings provide the first demonstration of the selective capacity of RNase L in intact cells and link this selective activity to cellular levels of 2-5A.

Differential display PCR analysis was used to identify mRNAs that were differentially expressed in N1E-vector and N1E-RNase-L cell lines and identified ISG43, ISG15 mRNA as negatively regulated by RNase L (Li et al, 2000). During the IFN-antiviral response in RNase L-null cells, PKR mRNA stability was enhanced, PKR induction was increased and the phosphorylated

form of eIF2α appeared with extended kinetics compared to similarly treated wild type cells. An enhanced IFN-response in RNase L-null cells was also demonstrated by monitoring inhibition of viral protein synthesis (Khabar et al, 2003). MyoD mRNA levels were decreased in C2 cells transfected with an inducible RNase L construct. The effect of RNase L activity on MyoD mRNA levels was relatively specific because expression of several other mRNAs was not altered in C2 transfectants (Bisbal et al, 2000). Le Roy and coworkers down-regulated RNase L activity in human H9 cells by stably transfecting (i) RNase L antisense-cDNA or (ii) RLI sense-cDNA constructs. In contrast to control cells, no post-transcriptional down-regulation of mitochondrial mRNAs and no cell growth inhibition were observed after IFN-α treatment in these transfectants. These results demonstratd that IFN-α exerts its antiproliferative effect on H9 cells at least in part via the degradation of mitochondrial mRNAs by RNase L. (Le Roy et al, 2001). Similarily Chandrashekaran and coworkers showed RNase-L-dependent decrease in mtDNA-encoded mRNA transcript levels in monensin-treated mouse embryonic fibroblasts (MEFs) (Chandrashekaran et al, 2004).

III.4.2. Antiviral immunity

Induction of RNA decay by RNase L is one of the host cell responses to viral infection. The most important line of evidence that link the 2-5A system to specific antiviral effects were obtained by measuring: (1) 2-5A accumulation and RNase L activation in virus-infected cells (Hearl and Johnston, 1987); (2) antiviral effects in cells expressing 2-5A synthetase cDNA (Schroder et al, 1992); and (3) enhanced virus production and reduction of the antiviral effects of IFN, caused by inhibiting RNase L activity in cells. For instance, it was shown that expression of the 40kDa form of human 2-5A synthetase from a cDNA in chinese hamster ovary (CHO) cells provided resistance to the picornavirus, mengo virus (Chebath et al, 1987). Similarly, expression of the 40kDa human 2-5A synthetase cDNA in a human glioblastoma cell line, T98G, and expression of murine 43kDa 2-5A synthetase from a cDNA in mouse NIH 3T3 cells resulted in resistance to EMCV replication (Rysiecki et al, 1989). Another strategy to study the

involvement of 2-5A/RNase L system in the antiviral activity of IFN was to use the 2-5A analog, $CH_3Sp(A2'p)2A2'pp3'OCH_3$, which binds to, but does not activate RNase L (Defilippi et al, 1985; Defilippi et al, 1986). Transfection of the analog into IFN-treated, EMCV-infected murine L929 cells inhibited rRNA cleavage and increased virus production by upto 10 fold. Hassel and coworkers (Hassel et al, 1993) showed that expression of a dominant negative truncated RNase L in murine SVT2 cells blocked the rRNA cleavage and reduced the anti-EMCV effects of IFN about 250-fold compared with the IFN-treated, vector control cells. The RNase L knockout mice succumbed to EMCV and HSV-1(McKrae strain) infections more rapidly than the infected wild type mice (Zhou et al, 1997). RNase L knockout mice treated with IFN prior to EMCV infection also died several days earlier than the wild type mice with the same treatment. However, IFN treatment extended survival against EMCV infection of both the RNase L-wild-type and knockout mice, indicating multiple and overlapping antiviral pathways of IFN.

So far, RNase L has been shown to have antiviral effects against many viruses such as EMCV, vaccinia virus, reovirus, herpes simplex virus (HSV) and SV40 (Baglioni et al, 1984; Diaz- Guerra et al, 1997; Rivas, 1998). Austin and coworkers (2005) evaluated resistance to HSV-1 in RNase L-deficient mice, treated with IFN-α6 and IFN-β transgenes. In the absence of RNase L, the antiviral effectiveness of the IFN-transgene was lost (Austin et al, 2005). When RNase L activity was down-regulated in West Nile Virus (WNV) resistant cells via stable expression of a dominant negative RNase L mutant, 5- to 10-times higher yields of WNV were produced (Scherbik et al, 2006). PKR and RNase L act as important effector molecules against WNV infection. Mice lacking PKR and RNase L were significantly more susceptible to WNV infection and showed increased viremia and viral burden in peripheral tissues, early entry into the brain, and higher viral loads in the CNS than the wild-type mice (Samuel et al, 2006). However, viral evasion of the 2- 5A/RNase L system was also reported. Vaccinia virus E3L proteins sequestered the dsRNA from 2-5A synthetase (Rivas et al, 1998), whereas reovirus S4 gene encodes a dsRNA-binding protein σ3 with the same function (Beattie et al, 1995).

III.4.3. Apoptosis

At the cellular level, the antiviral effects of IFN may be partly due to apoptosis. Indeed, activation of PKR and 2-5A synthetase by dsRNA have been shown to induce apoptosis. Several lines of studies link RNase L to apoptosis in cells in response to viral infection. RNase L-null mice showed enlarged thymuses and reduced levels of spontaneous apoptosis in both the thymus and spleen. In addition, thymocytes and lymphocytes from spleen of RNase L-null mice were resistant to apoptosis induced by staurosporine and irradiation (Zhou et al, 1997; Rusch et al, 2000). Furthermore, over expression of dominant negative RNase L (mouse RNase L lacking the C-terminal 89 a.a.) in cells reduced apoptosis whereas over expression of wild type RNase L enhanced apoptosis in response to viral infection (Hassel et al, 1993). Malathi and coworkers showed that RNase L-deficient prostate cancer cells are remarkably resistant to apoptosis induced by Topoisomerase I-inhibitors and tumor necrosis factor-related apoptosis-inducing ligand, TRAIL (Malathi et al, 2004). The apoptosis induced by RNase L involves cytochrome c release, it is caspase dependent, and inhibited by overexpression of Bcl-2 (Castelli et al, 1997; Rusch et al, 2000; Silverman, 2003). A study revealed that RNase L mediates virus-induced apoptosis through activating c-Jun NH_2-terminal kinase (JNK) (Li et al, 2004). Naito et al found that down regulation of RNase L inhibited apoptosis induced by 1-(3-C-ethynyl-ß-D-ribo-pentofuranosyl) cytosine (ECyd), which inhibits RNA synthesis through competitive inhibition of RNA polymerase I (Naito et al, 2006).

III.4.4. Antiproliferative effect

Introduction of 2-5A into cells results in an inhibition of the growth rate, suggesting a role of RNase L in antiproliferation (Hovanessian et al, 1980). Furthermore, RNase L and 2-5A synthetase levels were reported to be elevated in growth-arrested or differentiated cells and reduced in rapidly dividing cells, indicating that RNase L may be involved in fundamental control of cell proliferation and differentiation (Jacobsen et al, 1983; Krause et al, 1985). Cells expressing a dominant negative form of RNase L (mouse

RNase L lacking the C-terminal 89 a.a.) are resistant to the antiproliferative activity of IFN-α (Zhou et al, 1997).

III.4.5. Anticancer effect

Anticancer role of RNase L may be a collective effect of its antiviral, antiproliferative and apoptotic functions. The first *in vivo* evidence implicating RNase L as a tumor suppressor came from identification of *RNASEL* as the candidate gene for human prostate cancer 1 (HPC1) (Silverman, 2003). The direct evidence that RNase L is able to inhibit tumour growth *in vivo* was provided by Liu and coworkers (Liu et al, 2007). To directly measure the effect of RNase L on tumour growth in the absence of other IFN-induced proteins, human RNase L cDNA was stably expressed in P-57 cells, an aggressive mouse fibrosarcoma cell line. Three clonal cell lines were isolated in which the overexpression of RNase L was 15–20-fold higher than the endogenous level. Groups of five nude mice were subcutaneously injected with either the human RNase L overexpressing clones or the control cells transfected with an empty vector. Tumour growth by the two cell lines was monitored by measuring the tumour volumes. In the human RNase L overexpressing group, tumour formation was significantly delayed and the tumours grew much slower compared to the control group.

III.4.6 Stress response

As early as 1991, the role of stress in RNase L expression was indicated by Krause and coworkers, they observed increased level of RNase L in murine L929 cells after exposure to 2.45-GHz continuous-wave microwaves (SAR = 130 mW/g) (Krause et al, 1991). In our Laboratory, different stressors were used to study the expression of RNase L and apoptosis in human cervical carcinoma (HeLa) cells (Pandey, Bajaj and Rath, 2004). Chemotherapeutic agents like cisplatin, doxorubicin, vinblastin and vincristine showed RNase L-induction, RNA degradation and apoptosis. RNase L was also shown as oxidative stress-inducible, H_2O_2 and doxorubicin, a potent inducer of H_2O_2 in cells, also induced RNase L. RNase L was also induced by $CaCl_2$ and TNF-α.

III.4.7. Small RNA generation

Recently, Malathi and coworkers showed that activation of the antiviral endoribonuclease, RNase L, by 2'-5'-linked oligoadenylate (2-5A) produced small RNA cleavage products from self-RNA that initiated IFN production. Mice lacking RNase L produced significantly less IFN-β during viral infection than the infected wild-type mice (Malathi et al, 2007). This indicates RNase L is involved in RNA processing for the stimulation of innate immune response.

III.5. Interaction of RNase L with other proteins

III.5.1. RNase L Inhibitor (RLI)

In 1995, Bisbal and coworkers cloned a novel protein from the human lymphoid daudi cells, expression of this protein led to the inhibition of RNase L activity and hence named RNase L inhibitor (RLI) (Bisbal et al, 1995). RLI is an exceptionally conserved protein found in all eukaryotes and archaea sequenced so far (Gabaldon et al, 2004). For example, *Drosophila* ortholog *Pixie* and yeast *Rli1p* share 66% and yeast Rli1p and human RLI have 67% amino acid identities. RLI belongs to the ABCE subfamily of ABC proteins, which contain two nucleotide-binding domains and two N-terminal iron sulfur clusters. In contrast to most ABC domain proteins, members of this subfamily do not contain the membrane-spanning domains that would enable them to function as transporters (Kerr, 2004). RNase L is found in vertebrates, so the function of RNase L-inhibition by RLI does not account for conservation of RLI in invertebrates (Kerr, 2004). *Drosophila* ortholog of RLI, *Pixie* is known to interact with the translation initiation factor eIF3 and ribosomal protein. It was further observed that depletion of *pixie* resulted in impairment of translational initiation (Chen et al, 2006). RLI and its homologues are also thought to play a role in ribosome biogenasis, nuclear export, or both (Kispal et al, 2005). It has been found in the nuclei associated with the 40S and 60S subunits, as well as *Hcr1p*, a protein required for rRNA processing. It has been

shown that the iron-sulfur (Fe/S) clusters are necessary for ribosome biogenesis and/or nuclear export, although the exact mechanism is unknown.

III.5.2. eRF3/RNBP – link to translation

RNase L was shown to interact with RNA binding protein (RNABP) (Le Roy et al, 2000). RNABP was later identified as a translation termination release factor (*eRF3*) (Le Roy et al, 2005). After activation by 2-5A, RNase L can interact with *eRF3*. This association can either help to localize RNase L to its mRNA target or can modulate its function, but it is also a way to modulate *eRF3* activity. Importantly, the regulation of *eRF3* activity depends on the 2-5A oligomer size activating RNase L. Binding of 2-$5A_3$ or 2-$5A_4$ induces a conformational change in RNase L that promotes its interaction with eRF3. In one conformational change, the eRF3e RNase L interaction brings RNase L into close association with the mRNA, where it can act as an endoribonuclease. But binding with 2-$5A_3$ can induce another conformational change leading to an RNase L-*eRF3* complex that can modulate translation termination and promote ribosomal readthrough of a termination codon. Moreover, RNase L regulates the +1 frame shifting of the antizyme 1 mRNA in IFN-treated cells. This was the first report implicating a nuclease, RNase L, in the translational regulation of a cellular mRNA independent of its nuclease activity.

III.5.3. Interaction with Androgen Receptor

Functional crosstalk between IFN-signalling and dihydrotestosteron (DHT) was described by Bettoun and coworkers (Bettoun et al, 2005). They performed RNA microarray analysis to reveal an IFN-DHT antagonism in subset of genes. This effect was reproduced *in vitro* as IFN could antagonize the induction of a reporter gene by DHT in a cell type-specific manner. In an attempt to elucidate the mechanism underlying this cross-talk, co-immuno-precipitation and GST pulldown experiments were performed to show that RNase L interacted with androgen receptor (AR) in a ligand-dependent manner. In transient transfection experiment, overexpression of wild type or

R462Q mutated RNase L differentially affected the ability of IFN to antagonize DHT-mediated transactivation. Furthermore, it was also shown that IFN-insensitive cells could become sensitive to IFN upon down-regulation of AR-expression by siRNA. This finding also indicated how the AR and RNase L pathways may be involved in development of protate cancer since both the molecules have been implicated in prostate cancer progression.

III.6. RNase L and disease

III.6.1. Prostate cancer

The mammalian (human) prostate is a walnut sized secondary sexual accessory gland of the male reproductive system located beneath the bladder and in front of the rectum that produces secretions to the seminal fluid. Age, lifestyle-related factors, dietary factors, and androgen have long been recognized as contributors to the risk of prostate cancer. The Ribonuclease L has recently been identified as a candidate-gene for Hereditary Prostate Cancer 1 (*HPC1*) which is frequently associated with prostate cancer pathogenesis (Carpten et al, 2002). Interestingly, the prototype of these genes, *HPC1*, maps to the RNase L gene, *RNASEL* (Casey et al, 2002). Several germline mutations or variants in the *HPC1/RNASEL* gene have been observed among hereditary prostate cancer cases. A controlled sib-pair study implicated the RNase L R462Q variant in up to 13% of unselected prostate cancer cases (Casey et al, 2002). One and two copies of the mutated gene increased the risk of prostate cancer by about 150% and 200%, respectively. The RNase L ''Q'' variant at residue 462 in the kinase-like region had a 3X fold decrease in the catalytic activity compared to the wild-type enzyme, due to an impairment in dimerization (Xiang et al, 2003) However, while several case-controlled genetic and epidemiologic studies support the involvement of *RNASEL* (and notably the R462Q variant) in prostate cancer etiology others do not (Silverman, 2003) suggesting that population differences and environmental factors, such as viral infection, may modulate the impact of *RNASEL* on prostatic carcinogenesis. Therefore, there is a possibility that the linkage of RNase L alterations to *HPC* might reflect enhanced susceptibility to a viral

agent. To test this hypothesis, RNA samples derived from wildtype and RNase L variant (R462Q) prostate tumors were examined for evidence of viral sequences by hybridization to a DNA microarray composed of the most conserved sequences of all known human, animal, plant and bacterial viruses (Urisman et al, 2006). Because the array contains highly conserved sequences within viral nucleic acids, it can detect viruses not explicitly represented. These studies identified a novel retrovirus, xenotropic murine leukemia related virus (XMRV) in 8 (40%) of 20 R462Q homozygous prostate cancer tissues, and in 1 (1.5%) of 66 tissues that harbored at least one copy of the wild-type allele. Three of the complete XMRV genomes were sequenced, sharing >98% nucleotide and >99% protein sequence identity. The virus encodes four major proteins, gag, pro, pol, and env. XMRV is more closely related to the xenotropic and polytropic than to the ecotropic murine retroviruses. Complete viral genome sequences were obtained from three strains and partial sequences were obtained for another six XMRV strains. XMRV is a canonical gammaretrovirus, with gag, pro-pol and env genes, and is not closely related to any endogenous human retroviral (HERV) elements. In addition, XMRV sequences are not present in any human genome sequences that have been reported to date (Urisman et al, 2006). Soon after that Silverman's group constructed a complete infectious clone for XMRV strain VP62 (Dong et al, 2007). In the same study, XMRV provirus integration sites were mapped in DNA isolated from human prostate tumor tissue. These findings represented the first detection of xenotropic MuLV-like agents in humans, and revealed a strong association between infection with the virus and defects in RNase L activity.

III.6.2. Other cancers

Correlation of RNase L to prostate cancer encouraged to look for its role in other cancers. As prostate cancer occurs in some familial pancreatic families, Bartsch and co-workers evaluated the role of two variants of *RNASEL* gene: E265X and R462Q in the etiology of pancreatic cancer (Bartsch et al, 2005) The study showed that the *RNASEL* R462Q variant might be associated with an increased risk for sporadic pancreatic cancer and with

more aggressive tumors in familial pancreatic cancer. The R462Q variant of RNase L correlated with earlier age of onset of hereditary non-polyposis colorectal cancer (Kruger et al, 2005). Elevated bevels of RNase L in the tumors were observed compared to the corresponding normal mucosa. An monoclonal Antibody against RNase L revealed elevated amounts of this RNase in sections of the tumors, largely in the base of the villi (Wang et al, 1995).

III.6.3. Chronic Fatigue Syndrome

Chronic fatigue syndrome (CFS) is an illness characterized by long-lasting fatigue accompanied by non-specific symptoms. Several reports indicated the up-regulation of components of the 2-5A/RNase L pathway in extracts of peripheral blood mononuclear cells (PBMCs) from CFS patients as well as the accumulation of a low molecular weight 2-5A-binding protein of 37 kDa (Suhadolnik et al, 1997). This 37kDa protein could be a biochemical marker for CFS. The polypeptide is an apparent degradation product of the native RNase L due to an increased proteolytic activity in CFS PBMC extracts. An equivalent degradation of RNase L could be observed when recombinant RNase L was incubated with human leucocyte elastase *in vitro* (Demettre et al, 2002). The 2-5A trimer and tetramer binding appeared to stabilize RNase L in PBMC cell extracts from the CFS patients. These observations suggested that in CFS, there is increased proteolytic activity in the PBMC's causing accumulation of the 37 kDa polypeptide (Fremont et al, 2005).

III.7. RNase L expression

Expression of RNase L had been established in different tissues much before it was cloned or antibodies were raised against it. This was possible by radiolabeling of 2-5A. Presence of RNase L in rabbit liver, kidney, spleen and reticulocyte (Nilsen et al., 1981; Krause and Silverman, 1993) mouse liver, kidney, lungs, intestine, spleen, brain, testis, thymus, intestine and heart (Nilsen et al, 1981; Floyed-Smith and Denton, 1988; Silverman et al, 1988)

was shown in absence of IFN. RNase L is however, not found even in trace amounts, in murine neuroblastoma cell line, NIE115 (Silverman et al, 1986). RNase L peaks soon during postnatal development in many organs and gradually decreases as the animal ages (Floyed-Smith et al, 1988). Determination of RNase L using monoclonal antibody showed the presence of RNase L in normal colonic mucosa with elevated levels in the colorectal tumors and polyps (Wang et al, 1995). In 2005 Zhou and coworkers mapped the promoter of RNase L and also determined and compared RNase L levels in different human and rodent cancers and normal cell types using a radiolabeled 2-5A derivative. In addition, levels of RNase L were established in various normal human tissues and cell types by immunoblotting and immunohistochemistry (Zhou et al, 2005).

III.8. Evolution of RNase L

Taking advantage of the radiolabelled 2-5A binding assay for RNase L, many workers probed the presence of RNase L in different organisms. Intrestingly, the 2-5A binding activity was found only in higher vertebrates like mammals, aves and reptiles while no activity was found in fish, insects, plants, slime moulds and bacteria (Cayley et al, 1982). As soon as cloning of RNase L gene was performed, Bork and Sanders reported homology between RNase L and a evolutionary conserved yeast protein, *Ire1p*, which led to a prediction that yeast *Ire1p* is an endonuclease (Bork & Sanders, 1993) This prediction was later verified in studies with purified yeast *Ire1p* (Sidrauski & Walter, 1997). *Ire1p* is an integral membrane protein of the endoplasmic reticulum and an essential factor in mediating the unfolded protein response (UPR) in yeast, where it senses unfolded proteins in the lumen of the ER leading to splicing of the HAC1 mRNA, coding for the UPR-specific transcription factor (Sidrauski & Walter, 1997), *Ire1p* shows significant homology to RNase L and protein kinase domain of RNase L, while yeast *Ire1p* has both serine/threonine kinase and endoribonuclease activities, whereas, the RNase L have only RNase activity (Dong et al, 2001).

In 2004, Pandey and Rath observed that expression of recombinant human RNase L (1–741 a.a.) caused RNA degradation and inhibition of cell

growth in *Escherichia coli* even in absence of exogenous 2-5A. Upon computational analysis by pBLAST search, a putative transcription factor *yahD* from the *E. coli* genome showed highest homology with 90–259 a.a. region of human RNase L due to the ankyrin repeats with conserved GKT motifs (Pandey and Rath, 2004). Ankyrin repeats 2-4 (Tanaka et al, 2004) of RNase L are involved in 2-5A binding and dimerization. This study led to the postulation that *YahD* could interact with RNase L mimicking RNase L dimerization. It was also postulated that the ankyrin repeats region of RNase L and *YahD* may have common evolutionary origin.

IV. Materials and Methods

IV.1.1. Reagents

Acrylamide (30%)	29 g Acrylamide (Sigma, A9909) + 1 g N, N'-Methylene-bis-acrylamide (Sigma, M7256) dissolved in 60 ml H_20. Warmed on the magnetic stirrer to dissolve and made final volume to 100 ml, added 1g activated charcoal/100 ml acrylamide, stirred for an hour, filtered through Whatman 1MM filter paper, stored at 4°C in dark brown bottles. Bench life of 1 month.
Agarose gel	Agarose LE (Sigma, A9539). Typically 1.5 % Agarose gels in 0.5X TBE buffer were used with a final concentration of 0.5 µg/ml Ethidium bromide.
Aprotinin (1 mg/ml)	Protease inhibitor (Sigma A6279) Prepared in H_2O to a final concentration of 1 mg/ml and stored at –20°C.
APS (10%)	Ammonium per sulphate (Sigma, A-9164) 0.10 g APS was dissolved in 1 ml H_20 to get a 10% solution. Prepared fresh just before use.
Benzamidine (250 mg/ml)	Hydrochloride hydrate (Sigma, 6506) peptidase inhibitor. Prepared in H_2O at a concentration of 250mg/ml and stored at -20°C. Used to a final concentration of 0.5 mg/ml.
Bradford Reagent	Coomassie Brilliant Blue G-250 (s d fine, 54329). 10 mg dissolved in 5 ml ethanol + 10 ml conc. H_3PO_4 mix. Make volume to 100ml with distilled water.

BSA (10 mg/ml)	Bovine serum albumin (Fraction V) (Sigma, A9647). Dissolved 10 mg BSA in H_2O and stored as 1 ml aliquots at -20°C.
Chloroform	Qualigens Exela R. Stored at RT
DEPC	Diethyl pyrocarbonate (Sigma, D-5785) Stored at 4°C in dark bottles
DEPC-treated H_2O	0.1 % of DEPC added to double distilled water, mixed, allowed to stand at room temperature overnight, autoclaved for 30 min, cooled, stored at RT in cool, dry and RNase free condition
Developer (Photographic films)	(Kodak, 4908216). Dissolved 2.7g Part-B in 35.56 ml Part–A, made volume to 200 ml with water.
DTT (1M)	154.5 mg D-L-Dithiothretol (Sigma, D-9779) dissolved in 800 µl deionised H_2O and the volume made to 1 ml. Kept frozen as 100 µl aliquots at -20°C.
EDTA (0.5M)	Dissolved 93.05 g of disodium ethylene diamine tetraacetate. $2H_2O$ (Sigma, E5134) to 400 ml H_2O and adjusted pH to 8.0 with 40 gm NaOH pellets and 5 M NaOH, autoclaved and stored at room temperature.
EGTA (0.5M)	Ethylene glycol bis-[B-amino ethyl ether]- N, N, N', N' tetra acetic acid (Sigma, E4378). Suspended 1.902 gm of EGTA in 30-40 ml of sterile H_2O by warming on a magnetic stirrer. pH

	was adjusted to 7.0 by adding 10 M NaOH drop-wise while stirring. Made volume to 50 ml. Autoclaved and stored at room temperature.
Ethanol	(Merck-GR1.009830511), stored at 4°C.
Ethidium Bromide (10mg/ml)	Dissolved 100 mg ethidium bromide (Sigma, E-8751) in 10 ml sterile H_2O to make 10 mg/ml, stored as 1 ml aliquots at 4°C in Eppendorf tubes covered with aluminium foil.
Fixer	Dissolved 238 gm of X-ray acid fixing salts (Kodak, F 9000720) in 900 ml H_20. Filtered through Whatman 1mm filter paper and stored at room temperature in dark glass bottles.
Formaldehyde	Formaldehyde solution (37%) (Merk 61780805001046). Stored at RT.
Glycine	(Merck-GR 10420105001730). Stored at room temperature.
H_2O_2	Hydrogen peroxide. 30% purified solution (s d fine, 20366). Kept in dark bottles at 4°C. Made fresh dilutions in H_20 and discarded after use.
HCl (1N)	Hydrochloric acid. Added 8.25 ml of concentrated HCl (Sp. Gravity 1.19; approx. 12.1 N) to H_20 and made volume to 100 ml
Isopropanol	Isopropanol (s d fine, 20224). Stored at RT.
Leupeptin (1mg/ml)	Hydrochloride (Sigma, L9783). Serine and

	Cysteine protease inhibitor made in H_2O at a concentration of 1mg/ml and stored as 50µl aliquotes at -20°C.
Liquid nitrogen	Collected from the Central Instrument Facility, School of Life Sciences, J.N.U., New Delhi.
Loading Buffer (6X)	0.25% Bromophenol blue (Sigma, 17317EO), 0.25% Xylene cyanol FF (Sigma, X4126) in 30% glycerol (Merck, 10409405001730), stored as 1 ml aliquots at 4°C.
Lysis Buffer (whole tissue lysate)	50 mM Tris-Cl pH 7.5, 150 mM NaCl, 2 mM EDTA pH 8.0, 12 mM EGTA pH 7.5, 1 mM Sodium orthovanadate, 2 mM DTT, 1% NP-40, 0.5% Sodium deoxycholate (Sigma, D6750), 1 mM NaF (Sigma, S1504), 1 mM PMSF, 5 µg/ml Leupeptin, 5 µg/ml Aprotinin, 0.5 mg/ml Benzamidine. Made fresh before use.
β -Mercaptoethanol	β-Mercaptoethanol (14.4 M Merck-GR). Stored at 4°C.
Methanol	(Qualigens-ExcelaR), stored at RT in a dark bottle.
Membrane	Trans-Blot Transfer Medium: (Bio-Rad, 162-0115) Pure nitrocellulose membrane 0.45µm. Stored at RT in a clean and dry place.
Milk (non fat)	(C. D. H., 024363) Skim milk powder.
Normal Saline	0.9% NaCl solution in sterile H_2O. Autoclaved

	and used as ice cold.
NP-40 (10 %)	Sigma. 1-3021. IGEPAL CA-630. Nonionic detergent. (Octylphenoxy)polyethoxyethanol, chemically indistinguishable from Nonidet P-40. Dissolved 1 ml 100% Nonidet P-40 in 90 ml H_2O and mixed gently by inverting tube. Stored at RT
Nucleotides	dNTP mix, (Fermentas, R0181) 10 mM stock
PAGE	Polyacrylamide gel electrophoresis: Stacking gel: 5% Polyacrylamide in Tris-Cl pH, 6.8, Resolving gel: 8% Polyacrylamide in Tris-Cl, pH 8.8.
PBS,10X	1.3 M NaCl, 20 mM KCl, 78 mM $Na_2HPO_4.2H_2O$, 14 mM KH_2PO_4, pH adjusted to 7.4 with HCl, autoclaved and stored at RT.
PBST	1X PBS, pH 7.4 containing 0.1% Tween-20
PCR buffer (10X)	750 mM Tris-HCl, pH 9.0, 500 mM KCl, 200 mM $(NH_4)_2SO_4$. Stored as aliquots of 50 µl at -20°C.
PMSF	Phenylmethylsulfonylfluoride. (Sigma, P-7626) Dissolved 17.4 mg in 1 ml isopropanol to get a final concentration of 100 mM. Stored at -20°C.
Ponceu-S	100 mg Ponceu-S (Himedia, RM977) in 49 ml H_2O then added 1 ml acetic acid. Stored at RT
M-MLV RT (5X) reaction buffer	250 mM Tris-HCl (pH 8.3), 375 mM KCl, 15 mM $MgCl_2$ and 50 mM DTT. Stored as aliquots of 100 µl at -20°C.

Sample Buffer (2X) (SDS-PAGE)	100 mM Tris-Cl, pH 6.8, 4% (w/v) SDS, 0.2% (w/v) bromophenol blue, 20% glycerol, 200 mM DTT, in H_2O. DTT was added just prior to use. Stored at RT (otherwise SDS will precipitate). Shelf-life of 3 months.
SDS (10%)	Sodium dodecyl Sulphate (Sigma; L-4390). 10% (w/v) SDS was made in 50 mM Tris HCl, pH 8.0. Stored at RT.
Sodium acetate (3M, pH 5.0)	20.41 g Sodium acetate (Qualigens AR) was dissolved in 20 ml DEPC-treated H_2O and the pH was adjusted to 5.2 with glacial acetic acid. The volume was made upto 50 ml with DEPC-treated H_2O, autoclaved and stored at RT
TBE Buffer (5X)	54 gm Trizma base (Sigma, T6066), 27.5 gm boric acid and 20 ml 0.5 M EDTA, pH 8.0, in a total volume of 1L in H_2O, autoclaved and stored at RT.
TEMED	N, N, N', N', Tetramethylethylenediamine (Sigma, Y7024). Stored at 4°C in dark bottle.
Transfer Buffer (Western blot)	To prepare 1 liter of transfer buffer mix 2.9 g of glycine, 5.8 g of trizma base (Sigma, T6066), 0.37 g of SDS and 100 ml methanol. Stored at RT.
TRI – Reagent	Sigma, CAT T9424. Stored at 4°C.

Tris-Cl (0.5 M, pH 6.8)	(Sigma, T6066) 6.1 gm was dissolved in 80ml distilled H_2O, pH 6.8, volume made to 100 ml with H_2O. Autoclaved and stored at 4°C.
Tris.Cl (1.5 M, (pH 8.8)	(Sigma, T6066) 18.2 g was dissolved in 80 ml distilled H_2O, pH 8.8, volume made to 100 ml with H_2O. Autoclaved and stored at 4°C.
Tris-Glycine-SDS (5 X)	15.1 g Tris base (Sigma, T6066), 75.07 gm Glycine and 5g Lauryl Sulphate Sodium salt was dissolved in 800 ml H_2O and final volume made to 1 L. [Final concentration: 0.025 M Tris.Cl, 0.192 M Glycine, 0.1% (w/v) SDS, pH 8.3.
Triton X-100 :	(Sigma, T-8787), diluted to 10% in water and stored at RT.
Tween-20	Merck-GR. Stored at RT
Water	Double distilled autoclaved H_2O, deionized H_2O
Whatman Paper	Whatman 3 MM Paper (3030917), stored in a clean dry place
X-rays film	Kodak (Kodak XBT-5, 4909958), stored at RT in a cool and dry place.

IV.1.2. Enzymes

Reverse Transcriptase	MMLV Reverse Transcriptase (Promega, M1701, 200 U/µl), stored at -20°C.
rRNasin	(Promega, N2515) stored at -20°C 40 U/µl
Taq polymerase	(Biotools, 10.012, 1U/µl), stored at -20°C.

IV.1.3. Antibodies

Anti mouse RNaseL antibody	Polyclonal, raised in Rabbit against GST-RNase L (mouse) recombinant protein prepared by Mr. Ankush Gupta, Ph.D. student in our laboratory. stored at -20°C.
HRP-conjugated Secondary antibody	Anti Rabbit IgG raised in Goat conjugated to HRP (Sigma, A9167), stored at -20°C.

IV.1.4. Primers

S.No.	Primer Name	Primer Sequence	Length nt.(mer)	Amplicon size (bp)
1	5'GAPDH	5'ACCACAGTCCATGCCATCAC 3'	20	1+2=452
2	3'GAPDH	5'TCCACCACCCTGTTGCTGTA 3'	20	
3	Oligo dT	5'$(dT)_{15}$ 3'	15	
4.	RT 5' chm RNase L	5'CTGCAACCACAAAACATCTTAA TA 3'	24	4+5=644
5.	RT 3' nchm RNase L	5'AGATCTGGAAATGTCTTCTGAA AATA 3'	26	

All primers were dissolved at a concentration of 100µM (100 pmole/µl) and stored at -20^0C. Oligo dT was dissolved at a concentration of 500 ng/µl.

IV.2. METHODS

IV.2.1. Computational analysis

Computational analysis included: 1. BLAST analysis, 2. Sequence comparison using bl2seq tool of NCBI and align tool of EBI, 3: disorderednes analysis using DisEMBL, 4. Hydropathy plot using Bioedit tool.

IV.2.2. Sequences

Different sequences were downloaded and saved in FASTA (Pearson, 1988) format from ExPASy (**Expert Protein Analysis System**) proteomics server's UniProt Knowledgebase (Swiss-Prot and TrEMBL) (http://www.expasy.ch/), NCBI protein database, (http://www.ncbi.nlm.nih.gov/).

IV.2.3. Homology search with Genomes

Homology search for human RNaseL (hRNase L) protein sequence were carried out with different genomes using Basic Local Alignment Search Tool (BLAST) (Altschul et al, 1997) available online from NCBI. (http://www.ncbi.nlm.nih.gov/blast/Blast.cgi). The best matching sequences were manually looked for and marked (+) for the region of their similarity to various RNaseL domains (Ankyrin repeats, Protein kinase homology and RNase domain).

IV.2.4. Sequence alignment

Homologous sequences obtained from BLAST search were aligned using NCBI's bl2seq program (Tatiana et al, 1999, http://www.ncbi.nlm.nih.gov/blast/bl2seq/wblast2.cgi). The aligned sequences were manually looked for conserved amino acid residues. The Expect value (e-value), % identity and similarity were recorded. *Escherichia coli* RNases (protein) sequences were aligned with human RNaseL sequence using

European Bioinformatics Institutes (EBI) ALIGN program (http://www.ebi.ac.uk/emboss/align/index.html).

IV.2.5. Disordered regions

Disordered regions in the mouse and human RNase L were predicted by using DisEMBL 1.5 (Linding, 2003, http://dis.embl.de/). The algorithm parameters were Savitzky-Golay smoothing frame-8, minimum peak width-8, maximum join distance-4. Threshold value for REMARKS465 was 1.20 and for Hot Loops definition was 1.40. The corresponding disordered regions' sequences from the two molecules were compared and recorded.

IV.2.6. Hydropathy score

Hydropathy plot of human and mouse RNaseL was plotted using BioEdit Sequence Alignment Editor (Hall, 1999, http://www.mbio.ncsu.edu/BioEdit/bioedit.html).

IV.3. Expression analysis

IV.3.1. Mice and tissue collection

Twelve to fourteen weeks old swiss albino male mice (*Mus musculus*) were obtained from the Animal House facility of Jawaharlal Nehru University. The mice were sacrificed by cervical dislocation and liver, kidney, brain, prostate, testis and spleen tissues were quickly collected, washed in chilled normal saline and snap frozen in liquid nitrogen and/or processed directly.

IV.3.2. RT-PCR

IV.3.2.1. RNA Isolation

RNA was isolated from the mouse tissues using Tri-Reagent (Sigma, T9424). Fifty to hundred mg of tissue was crushed and powdered in liquid nitrogen using a mortar and a pestle. One ml of Tri-Reagent was added and the mixture was homogenized by homogenizer. Homogenized samples were incubated for 15 min at room temperature, 0.3 ml of chloroform was added and the mixture was vortexed vigorously for 15 sec. The mixture was further incubated at room temp for 15 min. Then the samples were centrifuged at 12,000xg for 15 min at 4°C. The homogenate was separated into three phases, the upper aqueous phase containing RNA, the interphase containing DNA and the lower organic phase containing protein. The upper aqueous phase was collected and again extracted with 0.3 ml of chloroform for further deprotenization. The aqueous phase was transferred in to a fresh tube, 0.5 ml of isopropanol was added and the mixture was inverted several times to mix thoroughly. The samples were kept at room temp for 10 min to allow the RNA to precipitate, and then centrifuged at 12,000xg for 15 min at 4°C. The supernatant was discarded and 1ml cold 75% ethanol was added to wash the RNA pellet, which was again centrifuged at 7500xg for 5 min at 4°C for recovery. The RNA pellet was air-dried and resuspended in DEPC-treated water. The RNA conc was spectrophotometrically determined at 260 nm taking 1O.D.= 40 µg/ml. The ratio at $A_{260\ nm}/A_{280\ nm}$, the λ scan spectrum from 200-300 nm and the agarose gel picture of the 28S and 18S rRNAs were used to determine the RNA quality.

IV.3.2.2. Reverse transcription

In 0.5 ml eppendorf tube, 500 ng oligo$(dT)_{15}$ primer and 1.0 µg RNA were denatured in DEPC-treated water in a total volume of 15µl for 5 min at 70°C in a thermocycler and chilled on ice immediately. Ten microliter of the reaction mix was added to the denatured RNA as follows:

Components	Stock conc.	Volume (µl)	Final conc.
DEPC-treated water	-	2.75	-
5X MMLV-RT Buffer	5X	5.00	1X
dNTP	10 mM	1.25	0.5 mM
RNasin	40 U/µl	0.5	20 U/µl
MMLV-RT	200 U/µl	0.5	100 U/reaction
Total vol.		10	

The sample was incubated in a thermal cycler at 37 °C for 60 min.

IV.3.2.3. PCR

The single-stranded cDNAs, synthesized as above, served as the template for PCR using gene-specific primers for mouse RNase L (mRNase L) and Glyceraldehyde 3-Phosphate Dehydrogenase (GAPDH). The composition of the reaction mix for the mRNase L and GAPDH PCR reactions were as follows:

Components	Stock conc.	Volume (µl) (mRNaseL)	Volume (µl) (GAPDH)	Final conc.
Deionized water	-	14.0	18.5	-
PCR buffer	10X	2.5	2.5	1X
$MgCl_2$	50 mM	1.0	1.0	2 mM
dNTP mix	10 mM	0.5	0.5	0.2 mM
Forward Primer	25 pmol/µl	0.5	0.5	12.5 pmol/reaction
Reverse Primer	25 pmol/µl	0.5	0.5	12.5 pmol/reaction
Taq polymerase	1 U/µl	1.0	0.5	1 U/reaction
cDNAs (1^{st} strand reaction)		5.0	1.0	
Total vol.		25.0	25.0	

The PCR conditions for RNase L and GAPDH were as follows:

Step 1: 95 ^{O}C, 5 min.
Step 2: 95 ^{O}C, 45 sec.] denaturation
Step 3: 60 ^{O}C, 45 sec.] annealing
Step 4: 72 ^{O}C, 1 min.] extension
Step 5: Repeat steps 2-4 for 35 cycles.
Step 6: 72 ^{O}C, 10 min.

IV.3.2.4. Agarose Gel Electrophoresis

The agarose conc used in the electrophoretic separation of DNA were chosen on the basis of the size of the PCR-amplified DNA. Agarose was melted in double distilled water by heating and was cooled to about 50°C, 5X TBE (45 mM Tris-borate and 1 mM EDTA, pH 8.0) was added to make 0.5X TBE before adding ethidium bromide upto 0.5 μg/ml. The molten agarose was poured into a gel tray with combs in place and allowed to solidify. DNA samples were loaded in 6X Gel Loading Buffer and electrophoresed in 0.5X TBE buffer at 25 mA for 1 h. The DNA was visualized using an UV transilluminator and photographed by AlphaImager 3400 gel documentation equipment, Integrated Density Value (IDV) calculated by AlphaImager software was used for quantification.

IV.3.3. Western Blot

IV.3.3.1. Tissue protein extract

Mouse liver, kidney, brain, prostate, testis and spleen (50-100 mg) were crushed and powdered using a mortar and a pestle in liquid nitrogen. Two ml of lysis buffer per 100 mg tissue was added and the tissue powder was reconstituted in lysis buffer for 20-30 min. on ice. The homogenate thus formed was sonicated at 18 micron (μ) for 10 sec, thrice with 1 min gap for

every cycle. The sonicated homogenate was centrifuged at 12000xg for 15 min at 4°C. The supernatant was collected, aliquoted into 0.5ml Eppendorf tubes and stored at -80°C.

IV.3.3.2. Protein Estimation

Bradford's method (Bradford, 1976) was used for estimation of protein conc. in the tissue extracts. A standard curve of BSA was made by using a serial dilution of BSA (1 µg/ml) from 0, 2, 4, 6, 8, 10, 12 µg in a final vol of 0.8 ml in 1.5 ml Eppendorf tubes. Each conc was taken in duplicates. Two hundred µl of 5X Bradford's reagent was added to each tube and allowed to react for 5 min. The O.D. was measured at 595 nm in a spectrophotometer. A standard curve was plotted for the mean $O.D._{595nm}$ to estimate the conc. of BSA. Two µl of the protein extract in 0.8 ml was added with 200µl of 5X Bradford reagent, O.D. at 595 nm was estimated using the standard curve.

IV.3.3.3. Sample preparation

The protein extract (100µg) was boiled with equal volume of 2X SDS-PAGE sample buffer (100 mM TrisCl, pH 6.8, 4% w/v SDS, 0.2% w/v bromophenol blue, 20% glycerol, 200 mM DTT, in H_2O) in boiling water bath for 5 min then chilled on ice.

IV.3.3.4. SDS-PAGE

Sodium Dodecyl Sulphate Polyacrylamide Gel Electrophoresis (SDS-PAGE) was carried out according to Laemeli's method (Laemeli, 1970). Stacking and resolving gel solutions were made as follows:

Solution component	Component volume (ml) for 8% resolving gel (10ml)	Component volume (ml) for 5% stacking gel (3ml)
H_2O	4.6	2.1
30% acrylamide mix	2.7	0.5
1.5 M Tris (pH 8.8)	2.5	-
1.0 M Tris (pH 6.8)	-	0.38
10% SDS	0.1	0.03
10% APS	0.1	0.03
TEMED	0.006	0.003
Total	10	3

The solution was swirled gently to avoid formation of bubbles and quickly added with freshly prepared 10% APS and TEMED, poured in sealed vertical glass plates (Bio-Rad miniprotean III apparatus), covered with thin layer of isopropanol. It was allowed to polymerize for 30 min at RT, and after polymerization, the upper layer of isopropanol was completely removed and 5% stacking gel solution was poured and the 1.5 mm thick comb was put in to make the wells. After the stacking gel was polymerized, the comb was removed and the slots were washed well with 1X gel buffers to remove any unpolymerized acrylamide. The gel was placed in the vertical gel apparatus ensuring that there was no air bubble trapped between the buffer and the bottom of the gel. The 100 μg tissue extract sample was loaded into the well and electrophoresed in 1X Tris-Glycine-SDS Buffer at 80V at RT till the bromophenol blue dye migrated out of the gel.

IV.3.3.5. Western blotting

The gel was trimmed to remove the stacking gel. The gel was washed with the transfer buffer (39 mM glycine, 48 mM Tris, .037% SDS, 10 or 20% methanol, pH 8.3) to remove SDS. The gel and the nitrocellulose membrane were sandwiched between two sheets of Whatman 3MM sheets and packed into the Western blotting apparatus cassette. The transfer was carried out by electroblotting at 40V in the transfer buffer overnight in the cold room with constant mixing of the buffer. The gel was removed and the nitrocellulose

membrane was stained with Ponceu-S. All the lanes with markers were visible. The markers were marked with a ball-point pen on the nitrocellulose membrane. The membrane was washed with PBST to remove the Ponceu-S, freshly washed in 1X PBST, incubated in 5% non fat milk in PBST for 3h at room temp with mild shaking. Then it was washed with 1X PBST gently and incubated with the primary antibody (anti-mouse RNase L antibody raised in rabbit) in 2.5% nonfat milk at 1:1000 dilution in 1X PBST for 4 h at room temperature. Then the membrane was washed in 1X PBST thrice, 10 min each on a rotating platform to wash away all non-specifically bound antibodies. The membrane was then incubated with Horseradish Peroxidase (HRP)-conjugated secondary antibody (anti rabbit IgG raised in goat) in 2.5% nonfat milk in 1X PBST for 2 h at room temp, again washed in 1X PBST thrice, 10 min each on the rotating platform to wash away all non-specifically bound antibodies.

IV.3.3.6. Developing

All the subsequent steps were carried out in a dark room with photographic safe light. In a clean container 1 ml ECL solution (equal volumes of ECL solution I and II) was added and swirled to mix, the blot was placed in the ECL solution mixture and swirled for 1min taking care to ensure that the entire blot is constantly in contact with the solution. The membrane was blotted on tissue paper to remove all extra ECL, wrapped in saran wrap and placed on intensifying screen and exposed to Kodak X-ray film for varying time, 5 sec, 30 sec, 1 min, 2 min or more and then developed the film with X-ray developing and fixing solution with intermediate wash in water. The film was dried and aligned with the blot and marked with the position of the markers. The image was obtained by scanning of the X-ray film. The blot was stored at 4°C.

V. Results

The present study on RNase L was focused on two aspects and the results are organized into two sections: computational analysis and expression analysis.

V.1. Computational analysis

Computational analysis of RNase L was carried out on following basis and to achieve the following objectives.

(1) RNase L is an interferon- and virus-inducible endoribonuclease of the vertebrates, which is not only functional under antiviral conditions but also under other cellular stress and metabolic conditions. Although, the interferon system developed well in reptiles, birds and mammals; interferon-like functional systems might have existed partly in other organism. Homology search by computational analysis may find out proteins with similarity to RNase L. (2) RNase L is a unique endoribonuclease from mammalian system, which also has a unique structural design. RNase L functions should depend on its interactions with cellular RNAs, small molecules and cofactors and other proteins. Therefore, structural design(s) of RNase L should indicate its interaction potentials. (3) Computational analysis of RNase L with other genomes may find proteins related to RNase L in a evolutionary time-scale and, therefore, may help understanding how the RNase L/2-5 A pathway might have evolved for antiviral as well as other functions in mammals. The computational analysis of RNase L included its homology/comparison with *E. coli* genome, *E. coli* ribonucleases, RNase domain with bacterial, protozoan, yeast, algal genome database, and comparison of human RNase L with mouse RNase L. Many interesting features/information were observed.

V.1.1. Evolutionary analysis

Since RNase L is a unique endoribonuclease with ankyrin repeats, which are usually for protein-protein interactions and it is regulated by unique 2,5' oligoadenylate (2-5 A) cofactor in an interferon- or virus-inducible

manner, this 2-5 A pathway must have evolved in many steps for survival of the higher organisms against viral infections as an adaptive mechanism during evolution. Therefore, evolutionary biology of RNase L structure, function and 2-5 A pathway should be an interesting aspect of the biology of the innate immunity of vertebrates, especially mammals.

V.1.1.1. Homology with *E. coli* genome

To begin with the evolutionary study of RNase L, one of the most commonaly studied and characterized bacterial organism, *Escherichia coli* genome was selected for homology search. To find out the conserved/homologous sequences to human RNase L, Basic Local Alignment Search Tool (BLAST) (Altschul et al, 1997) was carried out using blastp program. The human RNase L protein sequence (accession no Q05823) was used as the query to find out the matching sequences against non-redundant (nr) protein database of *E. coli* (taxid: 562). The search results are shown below as Table-1

Table1: BLAST results of human RNase L sequence with *E. coli*

Accession No.	Protein	E-value	Homology region		
			Ank	PKR	RNase
NP_752376.1	Hypothetical ANK-repeats protein yahD	6e-16	+		
NP_286054.1	putative transcription factor	7e-16	+		
NP_414852.1	predicted transcriptional regulator	7e-16	+		
YP_001457150.1	ankyrin repeat protein	7e-16	+		
YP_444030.1	hypothetical protein O2ColV186	3e-12	+		
BAA07749.1	unknown	0.25	+		
YP_001458841.1	hypothetical protein EcHS_A2169	0.29	+		
YP_001463948.1	hypothetical protein EcE24377A_2913	0.84	+		

+: Region of similarity, E-value: Expect value, Ank: Ankyrin repeat region, PKR: Protein kinase homology region, RNase: RNase region of RNase L

The first four sequences (NP_752376.1, NP_286054.1, NP_414852.1 and YP_444030.1) showed significant sequence similarity in the ankyrin repeats region of RNase L as evident from the E-value (Table 1). All these five sequences belonged to a single gene, named putative transcription factor YahD and showed almost same region of matching sequences. None of these sequences is characterized as per literature and genome database. No significant similarity to the protein kinase and RNase domain region was found.

V.1.1.2. Comparison of RNase L and *YahD*

The best matching sequence to RNase L in the *E. coli* genome, YahD, (previously reported by Pandey and Rath, 2004) sequence was compared with RNase L for the conserved functionally important residues (Fig. 5). According to Tanaka et al (2004), the 60th tryptophan residue (60W) in RNase L forms stacking interaction with the 3rd adenine ring of 2-5A. The 60W seems to be a part of the conserved motif, i. e., GWTPL. This motif is conserved in both RNase L and *E. coli* YahD proteins. Morever, the GKT motif of 7th ankyrin repeat in RNase L is also conserved in *YahD*. Tanaka et al (2004) also showed that the 126th phenylalanine (126F) in RNase L interacts with the adenine ring of the first AMP of 2-5A. Although this 126F is not conserved in *YahD*, it aligns to GKT motif, which is known to interact with adenine and guanine, in which conserved lysine residues interact with phosphate groups of the nucleotides (Saraste et al, 1990). This GKT motif of *YahD* may have evolved into GFT motif of RNase L for 2-5A binding. Moreover, the suggestion of the presence of 2',5'-olgoadenylates in *E. coli* (Brown and Kerr, 1985; Trujillo, 1987) also suggested presence 2-5A binding protein in *E. coli.*

V.1.1.3. RNase L and *E. coli* RNases

RNase L is an endoribonuclease, so it may have evolved from other RNases. To test this hypothesis, the sequences of seven known endoribonucleases were compared to human RNase L. The individual

```
Identities = 59/194 (30%), Positives = 94/194 (48%), Expect = 2e-14

                ANK3                                    ANK4
RNaseL  90   KNGATPFILAAIAGSVKLLKLFLSKGADVNECDFYGFTAFMEAAVYGKVKALKFLYKRGA  149
             KN    ++LAA  G +  +K  L+ G D+N CD  G TA   A++Y +   ++ L  GA
YahD     4   KNLPADYLLAAQQGDIDKVKTCLALGVDINTCDRQGKTAITLASLYQQYACVQALIDAGA   63

                                                        ANK5
RNaseL 150   NVNLRRKT----------------------KEDQERLRKGGATALMDAAEKGHVEVLKI  186
             ++N +  T                      K D   + + G   L  A EKGH+ ++K
YahD    64   DINKQDHTCLNPFLISCLNDDLTLLRIILPAKPDLNCVTRFGGVGLTPACEKGHLSIVKE  123

                ANK6                                                ANK7
RNaseL 187   LLDEMGADVNACDNMGRNALIHALLSSDDS-DVEAITHLLLDHGADVNVRGERGKTPLIL  245
             LL     +VN  +++G   L+ A++ +D     +AI  LLL+HGA  ++  + GKTPL L
YahD    124   LLAHTEINVNQTNHVGWTPLLEAIVLNDGGIKQQAIVQLLLEHGASPHLTDKYGKTPLEL  183

RNaseL 246   AVEKKHLGLVQRLL  259
             A E+    + Q L+
YahD    184   ARERGFEEIAQLLI  197


Identities = 35/94 (37%), Positives = 51/94 (54%), Expect = 6e-04

                ANK1                            ANK2
RNaseL  29   LIKAVQNEDVDLVQQLL-EGGANVNFQEEEGGWTPLHNAVQMS-----REDIVELLLRHG  82
             L  A +   + +V++LL     NVN Q    GWTPL  A+ ++      ++ IV+LLL HG
YahD    109   LTPACEKGHLSIVKELLAHTEINVN-QTNHVGWTPLLEAIVLNDGGIKQQAIVQLLLEHG  167

                ANK3
RNaseL  83   ADPVLRKKNGATPFILAAIAGSVKLLKLFLSKGA  116
             A P L  K G TP  LA  G  ++ +L ++ GA
YahD    168   ASPHLTDKYGKTPLELARERGFEEIAQLLIAAGA  201
```

Fig. 5 Sequence comparison of human RNase L and *E. Coli YahD* protein. Residues involved in 2-5A binding (according to Tanaka et al, 2004) (in bold and italics). 60W – conserved in *YahD*. 65N, 89K, 126F, 131E, 155R – not conserved in *YahD* of *E. coli*. 126F is not conserved in *YahD* but it compares to the GKT motif of *YahD* as GFT. 60W residue is conserved in both hRnase L and YahD. It forms the part of GWPTL motif similar to GKPTL motif. GKT motif of 7th ankyrin repeat is conserved in both RNase L and *YahD*. Ank: ankyrin.

comparison of these endoribonucleases with hRNase L using the program bl2seq of National Center for Biotechnology Information (NCBI) (Tatiana et al, 1999) showed 'no significant similarity'. Then Align Program [Needle (Global) method] of European Bioinformatics institute (EBI) (http://www.ebi.ac.uk/emboss/align/) was used. The highest identity and similarity of RNase L was found with Ribonuclease E (Table 2)

Table 2. Comparison of *E. Coli* endoribonucleases with human RNase L

S. No.	Ribonuclease	Accession No.	Identity (I) with hRNase L	Similarity (S) with hRNase L
1	Ribonuclease E	P21513	9.7	**17.7**
2	Ribonuclease I	P21338	8.0	13.9
3	Ribonuclease HII	Q8X8X6	6.5	10.3
4	Ribonuclease Z	Q8XCZ0	5.2	9.0
5	Ribonuclease HI	P0A7Y6	4.6	8.4
6	Ribonuclease 3	P0A7Y2	5.3	8.3
7	Ribonuclease P	P0A7Y8	3.9	7.2

V.1.1.4. RNase domain of RNase L in bacterial genomes

To find out if the RNase domain of RNase L has any homolog in the known bacterial genome sequences, the RNase domain (587-741aa) of RNase L was used as query against all completed bacterial genomes (http://www.ncbi.nlm.nih.gov/sutils/genom_table.cgi) available at NCBI. The BLAST results are shown in Table 3.

Table 3. Bacterial sequences showing significant homology with the RNase domain (587-741aa) of human RNase L

Accession no.	Protein	E- value
ZP_01733044.1	putative sulfatase	1.4
YP_001375927.1	lipoprotein, putative	1.4
YP_053741.1	trehalose-6-phosphate hydrolase	1.8
YP_001435934.1	exporter of the RND superfamily-like protein	4.0
YP_001419744.1	SpoIIE	4.0

From the table, it can be concluded that prokaryotes may not have any sequences significantly similar to the RNase domain of RNase L.

V.1.1.5. BLAST with Protozoon genome

Protein-Protein BLAST (blastp) analysis of RNase L with Known protozooan genomes yielded following results (Table 4)

Table 4. Proteins showing homology to hRNase L in protozoan database.

Accession no.	Protein	E-value	Homology to region		
			ANK	PKR	RNase
XP_643383.1	hypothetical protein	8e-19	+		
XP_635408.1	homeodomain (HOX) containing protein	2e-17	+		
XP_637278.1	hypothetical protein	2e-16	+		
XP_001463870.1	hypothetical protein	3e-16	+		
XP_001681539.1	hypothetical protein	3e-16	+		
XP_637214.1	SecG	3e-16	+		
XP_001684935.1	hypothetical protein	5e-16	+		
XP_001565281.1	ankyrin/TPR repeat protein	9e-16	+		
XP_646625.1	hypothetical protein	3e-15	+		
XP_001683531.1	ankyrin/TPR repeat protein	3e-15	+		
EAN81824.1	hypothetical protein	7e-15	+		
EDO81319.1	Kinase, NEK	1e-14	+		
XP_643729.1	hypothetical protein	1e-14	+		
XP_001562981.1	hypothetical protein	2e-14	+		
EAN83390.1	hypothetical protein	2e-14	+		
XP_647192.1	**putative endoribonuclease**	**3e-14**		+	+
XP_001566955.1	hypothetical protein	5e-14	+		
XP_001467179.1	hypothetical protein	6e-14	+		

+: Region of similarity, E-value: Expect value, Ank: Ankyrin repeat region, PKR: Protein kinase homology region, RNase: RNase region of RNase L

The most significant matches in this analysis are in the ankyrin repeat region. Ankyrin repeats are conserved sequences distributed widely across all superkingdoms including bacteria, archaea, and eukaryota. Morever, the E-values of the matches are similar to that of *YahD*. Intrestingly, a putative endoribonuclease (XP_647192.1) from *Dictyostelium* showed significant similarity to the protein kinase and RNase domain of human RNase L.

V.1.1.6. Human RNase L and Dictyostelium *IreA* (XP_647192.1)

The *IreA* (XP_647192.1, a putative protein serine/threonine kinase of *Dictyostelium discoideum* AX4) and human RNase L showed significant homology (Fig. 6). The catalytically important residues: 661D, 667A, 672H and 392K are conserved in both human RNase L and *IreA* while *IreA* do not have any significant similarity to the RNA binding and catalytic site of hRNase L. It does not show any significant similarity to the ankyrin repeats region. The comparison shows 22% identities with an E-value of $3e^{-14}$. The regions of homology are spread over 358-712 aa of RNase L with 570-978 aa of *IreA*. Since *Dictyostelium* is the beginning of multicellular organisms in the evolutionary time scale, *IreA* and RNase L may have common/similar origin.

V.1.1.7. BLAST with Yeast genome

Similarity of RNase L was probed in unicellular fungi, yeast genome sequence using blastp program of NCBI. The Table 5 shows the most significant matches to hRNase L.

V.1.1.8. Human RNase L and yeast Ire1p

Fig. 7 shows the sequence comparison of hRNase L and yeast *Ire1p*. The yeast *Ire1p* is established as a RNase L homologue (Dong et al, 2001). The RNase function function of *Ire1p* was predicted due to the finding that it showed homology to the RNase domain of RNase L (Bork & Sanders, 1993). The *Ire1p* is an endoribonuclease and kinase which is involved in the endoplasmic reticulum stress response (ER-stress) in yeast and mammalian

```
Identities = 93/420 (22%), Positives = 170/420 (40%), Expect = 3e-14

hRNaseL  358  IGKLKFFIDEKYKIADTSEGG--IYLGFYEKQEVAVKTFCEGSPR-AQREVSCLQSSREN  414
              IGKL+   +   KI  T   G  +Y G  E ++VAVK       + A REVS L  S E+
IreA     570  IGKLEIITN---KILGTGSCGTIVYEGKMEGRKVAVKRMLSQFVKFADREVSILIHSDEH  626

hRNaseL  415  SHLVTFYGSESHRGHLFVCVTLCEQTLEACLDV-----------------------HRGE  451
              +++V +Y  E     +++ ++ C+++L+  +                        + G
IreA     627  TNVVRYYAKEEDDEFIYLAISFCQKSLDMYVQQTLSLQISPTDSPSIQSSNNNGNGNNGN  686

hRNaseL  452  DVENEE---DEFARNVLSSIFKAVQELHLSCGYTHQDLQPQNILIDSKKAAHLADF----  504
              +  N +   D   + ++  +FK ++ LH S    H+D++P N+LID      ++D
IreA     687  NNNNNQIIIDNKTKQMILELFKGLEHLH-SLNIVHRDIKPHNVLIDPNNRVKISDMGLGK  745

hRNaseL  505  -----DKSIKWAGD-----PQEV---------KRDLEDLGRLVLYVVKKGSISF------  539
                   D+S+ +  D     P E          K D+  LG +V Y++  G+  F
IreA     746  LLDNDDQSLTFTSDSHGWQPAEYLNGTNRNTKKVDIFSLGCVVYYLL-TGAHPFGHRYNR  804

hRNaseL  540  EDLKAQSNEEVVQLSPDEETKDLIHRLFHPGEHVRDCLSDLLGHPFFWTWESRYRTLRNV  599
              E    +   ++ Q+    +   L+H +       R  + + + HPFFW    +   L  V
IreA     805  EKNVLKGKFDIDQIKHLPDIHQLVHSMIQFEPEKRPDIGECINHPFFWEVHKKLSFL--V  862

hRNaseL  600  GNESDIKTRKSESEILRLLQPGPSEHSKSFDKWTTKINECVMKKMNKFYEKRGNFYQNTV  659
                   ++  K  S +   +        +     W  KI++ ++  + ++ +  G     ++
IreA     863  AASDYLEFEKPTSPLNLEIDSHVDLVTDGSGDWWLKIDQVLIDNIGRYRKYNG----KSI  918

hRNaseL  660  GDLLKFIRNLGEH---IDEEKHKKMKLKIGDPSLYFQKTFFDLVIYVY----TKLQNTEY  712
               DLL+ IRN   H   +  E+   + +       YF   FP L I  Y      L+N +Y
IreA     919  RDLLRVIRNKFNHYRDLSPEEQTCLGILPDGFFNYFDLKFPQLFIVTYLFILKNLKNDQY  978
```

Fig.6 Comparison of *IreA* (XP_647192.1), a putative protein serine/threonine kinase [*Dictyostelium discoideum* AX4] with human RNase L. Catalytically important residues 661D, 667A, 672H and 392K (bold letters) are conserved in both human RNase L and *IreA*. RNase L: 395-444 Zinc Finger, 587-741 Rnase. This protein was obtained after BLAST of human RNase L sequence with protozoan database (http://www.ncbi.nlm.nih.gov/sutils/blast_table.cgi?taxid=Protozoa)

```
Identities = 50/200 (25%), Positives = 84/200 (42%), Expect = 3e-05

RNaseL 520   DLEDLGRLVLYVVKKGSISFEDLKAQSNEEVVQL-SPDE-----------ETKDLIHRLF  567
             D+  +G +  Y++ KG   F D  ++ +  +  + S DE           E  DLI ++
Irelp  902   DIFSMGCVFYYILSKGKHPFGDKYSRESNIIRGIFSLDEMKCLHDRSLIAEATDLISQMI  961
             ____________________________________________________________
             PK Domain

RNaseL 568   HPGEHVRDCLSDLLGHPFFWTWESRYRTLRNVGNESDIKTRKSESEILRLLQPGPSEHSK  627
                   R     +L HP FW    +   L  V +  +I+ R   S +L     G
Irelp  962   DHDPLKRPTAMKVLRHPLFWPKSKKLEFLLKVSDRLEIENRDPPSALLMKFDAGSDFVIP  1021
             _____________________ _____________________________________
                                   Rnase domain

RNaseL 628   SFDKWTTKINECVMKKMNKFYEKRGNFYQNTVGDLLKFIRNLGEHIDEEKHKKMKLKIGD  687
             S D WT K ++  M  + ++ +    ++ + + DLL+ +RN   H  +       +L
Irelp  1022  SGD-WTVKFDKTFMDNLERYRK----YHSSKLMDLLRALRNKYHHFMDLPEDIAELMGPV  1076
             ____________________________________________________________

RNaseL 688   PS---LYFQKTFPDLVIYVY  704
             P     YF K FP+L+I VY
Irelp  1077  PDGFYDYFTKRFPNLLIGVY  1096
             ____________________

Identities = 36/137 (26%), Positives = 70/137 (51%), Gaps Expect = 0.005

                                                ZINC FINGER
RNaseL 365 IDEKYKIADTSEGGIYLGFYEKQEVAVKT----FCEGSPRAQREVSCLQSSRENSHLVTF  420
           + EK     +S   ++ G ++ + VAVK     FC+    A  E+  L  S ++ +++ +
Irelp  675 VSEKILGYGSSGTVVFQGSFQGRPVAVKRMLIDFCD---IALMEIKLLTESDDHPNVIRY  731

           ____________________________
RNaseL 421 YGSESHRGHLFVCVTLCEQTLEACLDVHR--GEDVENEEDEFARNVLSSIFKAVQELHLS  478
           Y SE+    L++ + LC   L+  ++      E+++ +++    ++L  I   V  LH S
Irelp  732 YCSETTDRFLYIALELCNLNLQDLVESKNVSDENLKLQKEYNPISLLRQIASGVAHLH-S  790

RNaseL 479 CGYTHQDLQPQNILIDS  495
               H+DL+PQNIL+ +
Irelp  791 LKIIHRDLKPQNILVST  807
```

Fig. 7 Sequence homology of human RNase L and Yeast *Ire1p*. Catalytically important residues: 661D, 667A, 672H and 392K (bold letters) are conserved in both human RNase L and Yeast *Ire1p*. RNase L: 395-444 Zinc Finger, 587-741: RNase.

cells, and has been linked to restoration of misfolded proteins (Tirasophon et al, 1998). This indicates that RNase L may also be involved in the stress response in relation to ER and protein translation compartments.

Table 5. BLAST analysis of hRNase L in *Saccharomyces cerevisiae* RefSeq proteins.
(http://www.ncbi.nlm.nih.gov/sutils/genom_table.cgi?organism=fungi)

Accession no.	Protein	E-value	Homologous Region		
			ANK	PKR	RNase
NP_012154.1	Subunit of the Set3 complex	1e-10	+		
NP_010550.1	Palmitoyl transferase	8e-09	+		
NP_014677.1	Ankyrin repeat-containing protein	1e-08	+		
NP_011946.1	**Serine-threonine kinase and endoribonuclease Ire1p**	**4e-08**		+	+
NP_011748.1	Regulatory, non-ATPase subunit of the 26S protein	1e-07	+		
NP_010015.2	Putative serine/threonine protein kinase	1e-06		+	
NP_013784.1	Component of a complex containing the Tor2p	4e-05	+		
NP_011606.1	Ser/Thr kinase involved in transcription	5e-05		+	
NP_014428.1	MAP kinase kinase kinase	9e-05		+	

+: Region of similarity, E-value: Expect value, Ank: Ankyrin repeat region, PKR: Protein kinase homology region, RNase: RNase region of RNase L

V.1.1.9. BLAST with algal genome

The newly sequenced genome of unicellular algae, *Ostreococcus lucimarinus* (Palenik et al, 2007) was searched for homlogous sequences to RNase L. The following sequences showed most significant similarities (Table 6)

Table 6. BLAST analysis of RNase L protein with the green algae *Ostreococcus lucimarinus.* (http://www.ncbi.nlm.nih.gov/genome/seq/BlastGen/BlastGen.cgi?taxid=242159)

Accession no.	Protein	E- value	Homology to region		
			ANK	PKR	RNase
XP_001421322.1	predicted protein	2e-14	+		
XP_001417922.1	predicted protein	3e-13	+		
XP_001416089.1	predicted protein	8e-12		+	+
XP_001421093.1	predicted protein	7e-11	+		
XP_001417444.1	predicted protein	2e-10	+		
XP_001421044.1	VIC family transporter	6e-10	+		
XP_001415679.1	predicted protein	2e-09	+		

+: Region of similarity, E-value: Expect value, Ank: Ankyrin repeat region, PKR: Protein kinase homology region, RNase: RNase region of RNase L

V.1.1.10. RNase L and algal homologue

Out of most significant matching sequences one protein sequence (XP_001416089.1) from the algal genome showed similarity to the RNase and protein kinase domains of RNase L. This sequence has certain conserved residues (661D, 667A, 672H and 392K) of human RNase L which are essential for the RNase function of RNase L (Fig. 8). This indicates that this algal protein may be related to RNase L.

V.1.2. Comparative analysis of human RNase L with mouse RNase L

V.1.2.1 Sequence comparison

The Fig. 9 shows homology of human and mouse RNase L sequences. The sequences show 65% identity and 78% positivity. Residues involved in 2-5A binding (60W, 65N, 89K, 126F, 131E, 135R), two P-loop motifs (GKT), RNase activity (392K involved in dimerization, 661D, 667R, 672H) and

```
Identities = 77/368 (20%), Positives = 146/368 (39%), Expect = 8e-12

RNaseL          379  IYLGFYEKQEVAVKTF-CEGSPRAQREVSCLQSSRENSHLVTFYGSESHRGHLFVCVTLC
                     ++ G  + + VAVK    +    A++E+  L +S E+ +++  +  E     +++ + LC
XP_001416089    30   VFEGELDGRRVAVKRLLAQFHELARKELQALIASDEHPNILRCFALEEDSNFVYMALELC

RNaseL          438  EQTLEACLDVHRGEDVENEEDEFARNVLSSIFKAVQELHLSCGYTHQDLQPQNILIDSKK
                                          ++L  +   +  LH   G  H+DL+PQN+LI S
XP_001416089    90   A-----------------------SILHDVVAGLAALH-GQGIIHRDLKPQNVLITSSG

RNaseL          498  AAHLADFDKSIK---------------------------WAGDP------QEVKRDLEDL
                        +AD   + +                         W          Q    D+  L
XP_001416089    125  RGKIADMGLAKRVNVSEGTSFYTHTNGNLNVNDAAGTSGWQAPERLTQGRQSRSVDVFSL

RNaseL          525  GRLVLYVVKKGSISF-EDLKAQSNE-----EVVQLSPDEETKDLIHRLFHPGEHVRDCLS
                     G L+ Y +  G+  F E L+  +N      +V +L    E + L+          R   +
XP_001416089    185  GCLMYYCLTGGAHPFGERLQRDANVVANSYDVSKLKYFPEAEALVKACIDADPSKRPSAT

RNaseL          579  DLLGHPFFWTWESRYRTLRNVGNESDIKTRKSESEILRLLQPGPSEHSKSFDKWTTKINE
                     ++L HP +W  E + + L +  +  +++ R S+  +LR  +   ++ S + D WT K++
XP_001416089    245  EILAHPMWWDAEKKLQFLIDASDRVELEDRMSDRSLLRAFET-RAKSSIACDDWTKKLDA

RNaseL          639  CVMKKMNKFYEKRGNFYQNTVGDLLKFIRNLGEHIDEEKHKKMKLKIGDPS---LYFQKT
                      +++ + ++ E  G     ++ DLL+ IRN   H  E   K  +     P     Y
XP_001416089    304  ALLENLGRYREYDG----TSLRDLLRVIRNKANHYRELPPKLQRTLGSYPDGLWRYVSIR

RNaseL          696  FPDLVIYV
                     FP L++ V
XP_001416089    360  FPALLLGV
```

Fig.8 Comparison of hRNaseL protein with the green algae *Ostreococcus lucimarinus* protein XP_001416089.1. Catalytically important residues: 661D, 667A, 672H and 392K (bold letters) are conserved in both RNase L and XP_001416089.1.

```
Identities = 470/719 (65%), Positives = 565/719 (78%), Expect = 0.0

                                        ANK1
Human   1    MESRDHNNPQEGPTSSSGRRAAVEDNHLLIKAVQNEDVDLVQQLLEGGANVNFQEEEGGW  60
             ME+ D+N PQ G  S+  +R  VED+  LIKAVQ  DV  VQQLLE GA+ N  E+  GW
Mouse   1    METPDYNTPQGGTPSAGSQRTVVEDDSSLIKAVQKGDVVRVQQLLEKGADANACEDTWGW  60
             ANK2                          ANK3
Human   61   TPLHNAVQMSREDIVELLLRHGADPVLRKKNGATPFILAAIAGSVKLLKLFLSKGADVNE  120
             TPLHNAVQ  R DIV LLL HGADP  RKKNGATPFI+A I G VKLL++ LS GADVNE
Mouse   61   TPLHNAVQAGRVDIVNLLLSHGADPHRRKKNGATPFIIAGIQGDVKLLEILLSCGADVNE  120
             ANK4                                  ANK5
Human   121  CDFYGFTAFMEAAVYGKVKALKFLYKRGANVNLRRKTKEDQERLRKGGATALMDAAEKGH  180
             CD  GFTAFMEAA  G  +AL+FL+ +GANVNLRR+T +D+ RL++GGATALM AAEKGH
Mouse   121  CDENGFTAFMEAAERGNAEALRFLFAKGANVNLRRQTTKDKRRLKQGGATALMSAAEKGH  180
                                ANK6
Human   181  VEVLKILLDEMGADVNACDNMGRNALIHALLSSDDSDVEAITHLLLDHGADVNVRGERGK  240
             +EVL+ILL++M A+V+A DNMGRNALI  LL+ D  +VE IT +L+ HGADVNVRGERGK
Mouse   181  LEVLRILLNDMKAEVDARDNMGRNALIRTLLNWDCENVEEITSILIQHGADVNVRGERGK  240
             ANK7                          ANK8
Human   241  TPLILAVEKKHLGLVQRLLEQEHIEINDTDSDGKTALLLAVELKLKKIAELLCKRGASTD  300
             TPLI AVE+KH GLVQ LL +E I I+  D++GKTALL+AV+ +LK+I +LL ++GA
Mouse   241  TPLIAAVERKHTGLVQMLLSREGINIDARDNEGKTALLIAVDKQLKEIVQLLLEKGADK-  299
             ANK9
Human   301  CGDLVMTARRNYDHSLVKVLLSHGAKEDFHPPAEDWKPQSSHWGAALKDLHRIYRPMIGK  360
             C DLV  ARRN+D+ LVK+LL + A  D  PPA DW P SS WG ALK LH + RPMIGK
Mouse   300  CDDLVWIARRNHDYHLVKLLLPYVANPDTDPPAGDWSPHSSRWGTALKSLHSMTRPMIGK  359
                                                ZINC FINGER
                  PROTEIN KINASE HOMOLOGY
Human   361  LKFFIDEKYKIADTSEGGIYLGFYEKQEVAVKTFCEGSPRAQREVSCLQSSRENSHLVTF  420
             LK FI + YKIA TSEG +YLG Y+ +EVAVK F E SPR  +EVSCL+   ++S+LV F
Mouse   360  LKIFIHDDYKIAGTSEGAVYLGIYDNREVAVKVFRENSPRGCKEVSCLRDCGDHSNLVAF  419

Human   421  YGSESHRGHLFVCVTLCEQTLEACLDVHRGEDVENEEDEFARNVLSSIFKAVQELHLSCG  480
             YG E  +G L+VCV+LCE TLE  L + R E VEN ED+FA ++L SIF+ VQ+LHL  G
Mouse   420  YGREDDKGCLYVCVSLCEWTLEEFLRLPREEPVENGEDKFAHSILLSIFEGVQKLHLH-G  478

Human   481  YTHQDLQPQNILIDSKKAAHLADFDKSIKWAGDPQEVKRDLEDLGRLVLYVVKKGSISFE  540
             Y+HQDLQPQNILIDSKKA  LADFD+SI+W G+ Q V+RDLEDLGRLVLYVV KG I FE
Mouse   479  YSHQDLQPQNILIDSKKAVRLADFDQSIRWMGESQMVRRDLEDLGRLVLYVVMKGEIPFE  538
                                                        RNASE
Human   541  DLKAQSNEEVVQLSPDEETKDLIHRLFHPGEHVRDCLSDLLGHPFFWTWESRYRTLRNVG  600
              LK Q++E ++ +SPDEETKDLIH LF PGE+V++CL DLLGHPFFWTWE+RYRTLRNVG
Mouse   539  TLKTQNDEVLLTMSPDEETKDLIHCLFSPGENVKNCLVDLLGHPFFWTWENRYRTLRNVG  598

Human   601  NESDIKTRKSESEILRLLQPGPSEHSKSFDKWTTKINECVMKKMNKFYEKR-GNFYQNTV  659
             NESDIK RK +S++LRLLQ    E  +SFD+WT+KI++ VM +MN FYEKR  N YQ+TV
Mouse   599  NESDIKVRKCKSDLLRLLQHQTLEPPRSFDQWTSKIDKNVMDEMNHFYEKRKKNPYQDTV  658

Human   660  GDLLKFIRNLGEHIDEEKHKKMKLKIGDPSLYFQKTFPDLVIYVYTKLQNTEYRKHFPQ  718
             GDLLKFIRN+GEHI+EEK + MK  +GDPS YFQ+TFPDLVIY+Y KL+ TEYRKHFPQ
Mouse   659  GDLLKFIRNIGEHINEEKKRGMKEILGDPSRYFQETFPDLVIYIYKKLKETEYRKHFPQ  717
```

Fig. 9 Comparison of hRNaseL (Q05823) and mRNaseL (Q05921). Residues involved in 2-5A binding (60W, 65N, 89K, 126F, 131E, 135R), two P-loop motifs (GKT), RNase activity (392K involved in dimerization, 661D, 667R, 672H) and binding and cleavage of RNA (712Y, 716F) are conserved. 462R (mutation at this position to Q is associated with prostate cancer) is replaced by H. +:similar aa.

binding and cleavage of RNA (712Y, 716F) are conserved. The 462R (mutation at this position to Q is associated with prostate cancer) in human RNase L is replaced by H in mouse RNase L. Overall, with respect to 2-5A cofactor binding, dimerization, RNA substrate binding and RNA cleavage, mouse RNase L and human RNase L are highly homologous.

V.1.2.2. Disordered regions in human RNase L and mouse RNase L

In order to understand the possible small regions which may contribute to flexibility or folding, disordered regions were studied in RNaseL. Disordered regions in RNase L (human and mouse) were found by using DisEMBL program and according to REMARKS 465 definition and Hot-loops definition (Linding et al, 2003, http://dis.embl.de/) are shown in Table 7.

Table 7. Disordered regions in human RNase L and mouse RNase L using DisEMBL (http://dis.embl.de/). Bold and italicized sequences are homologous sequences disordred in both mouse and human RNase L.

	hRNase L	mRNase L
Region disordered by REMARKS 465 definition	***1MESRDHNNPQEGPTSSSGRR20***	***1METPDYNTPQGGTPSAGSQRTVVE24***
	398SPRAQREVSCLQSSR412	----
	622PSEHSKSF629	----
	729GAGGASGLASPGC741	----
Regions disordered by Hot-loops definition	*1**MESRDHNNPQEGPTSSSGRRA**21*	*1**METPDYNTPQGGTPSAGSQRT**21*
	----	84DPHRRKKNGAT94
	*145**YKRGANVNLRRKTKEDQERL**164*	*147**KGANVNLRRQTTKDKRRLK**165*
	*226**LDHGADVNVR**235*	*227**QHGADVNVRG**236*
	265EINDTDSDGK274	----
	293CKRGASTDCG302	----
	329FHPPAEDWKPQS 340	----
	----	395ENSPRGCKEVSCLRDCGD412
	*506**KSIKWAGDPQEVKRDLEDL**524*	*506**IRWMGESQMVRRDL**519*
	*537**ISFEDLKAQSNEEVVQL**553*	*534**EIPFETLKTQNDE**546*
	*597**RNVGNESDIKTRKSESEILRLLQ PGPSEHSKSFDK**631*	*595**RNVGNESDIKV**605*
		*617**QHQTLEPPRSFDQWTS**632*
	----	646YEKRKKNPYQDT657
	----	678RGMKEILGDPSRYFQETF695
	----	713KHFPQPPPRLSVPEAVGPGGIQS735

V.1.2.3. Hydropathy Plot

In order to understand small regions, which may contribute to hydrobhobic patches in RNase L, Kyte and Doolittle Hydropathy plot (Hall, 1999) (http://www.mbio.ncsu.edu/BioEdit/bioedit.html) for human RNase L and mouse RNase L was compared. Fig.10, shows the overlapping hydrophobicity curve of both RNase L. The hydropathy plots show that both RNase L molecules have hydrophilic and hydrophobic regions alternating with each other from 1-710 aa. There are 14 regions of hydrophobicity upto 590 aa, the rest of the C-terminal region (590-741 aa) is more or less hydrophilic. Most of these hydrophobic regions overlap between mouse RNase L and human RNase L, except the region three (120-145 aa), which is different between the two RNase L molecules. Since this region partly falls into the 4^{th} ankyrin repeat, which binds 2-5A cofactor, hypothetically this difference between the mRNase L and hRNase L may result into certain conformational differences, which may result into differences in cofactor binding, hence dimerization and activation of RNase L.

V.2. Expression analysis

V.2.1. Mouse RNase L mRNA expression

The PCR reaction for the mouse and human RNase L cDNAs were optimized by Mr. Ankush Gupta, Ph.D student in our laboratory. The RT-PCR reaction was optimized using mouse liver total RNA preparations by him. To find the RNA expression profile of RNaseL in normal mouse tissues, RT-PCR in five mouse tissues, e. g., liver, kidney, brain, testis, and spleen was carried out (Fig. 11). The level of mRNA was measured by densitometric estimation of the RT-PCR product (band) of RNaseL divided by that of the GAPDH in terms of normalized ratio of the integrated density value (IDV). Maximum expression was observed in the spleen, while it was not detectable in the kidney. The liver and brain showed nearly comparable expression levels while the testis showed slightly higher than the liver and brain but lower than the

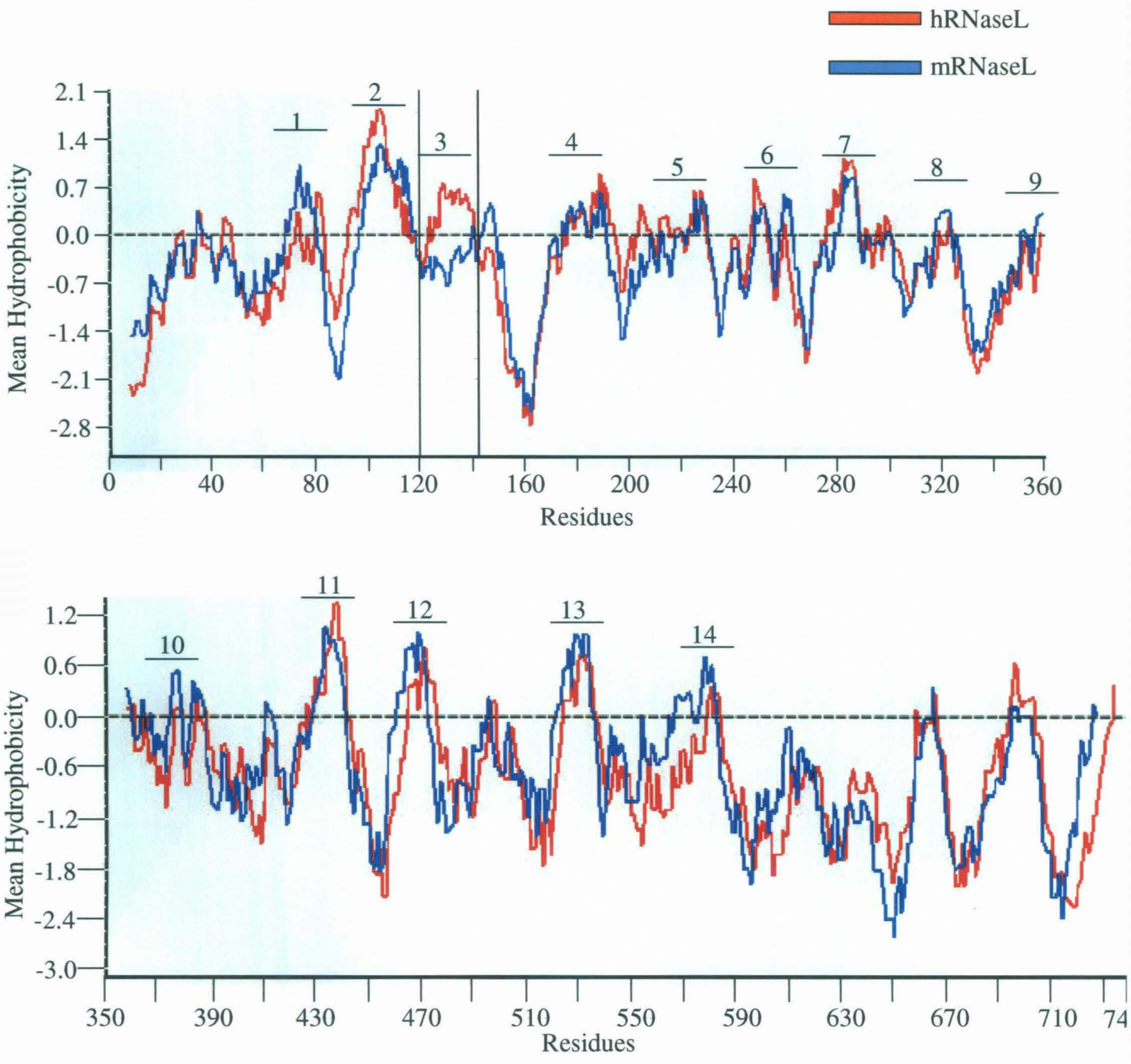

Fig. 10 Kyte and Doolittle scale mean hydrophobicity profile plot (Window seize = 15). Regions marked 1-14indicates hydrophobic regions from N-terminus to C-terminus, alternating with neighboring hydrophilic regions. The region 3 shows diffrence between human RNase L (hRNase L) and mouse RNase L (mRNase L)

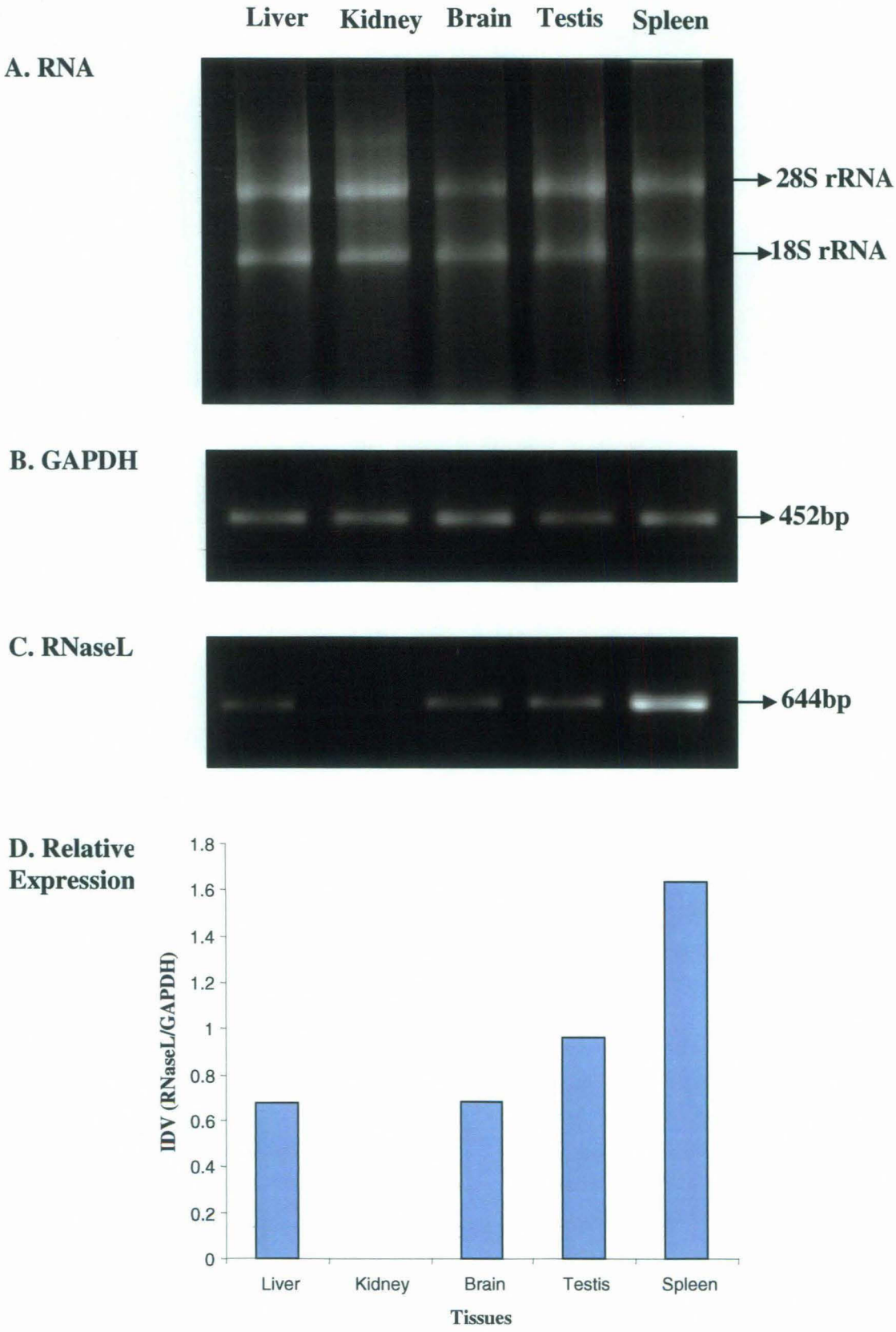

Fig.11. Total RNA and RT-PCR for RNase L mRNA expression in mouse tissues. A. Total RNA of different tissues; liver, kidney, brain, testis and spleen of the mouse **B**. RT-PCR using GAPDH primers to amplify a 452 bp amplicon. **C**. RT-PCR using RNase L primers to amplify a 644 bp amplicon. **D**. Relative Lavels of RNase L mRNA expressed as the normalised ratio of IDV of RNase L/ IDV of GAPDH.

spleen. This showed differential expression of RNase L mRNA in the mouse tissues.

V.2.2 Expression of mouse RNase L protein

Expression of mouse RNaseL protein was measured by western blot by using anti mouse RNase L polyclonal rabbit anti-serum against the recombinant mouse RNase L protein, both developed by Mr. Ankush Gupta Ph.D. student in our laboratory. The western blot protocol was also developed by him. Six normal mouse tissues i.e. liver, kidney, brain, prostate, testis, and spleen were studied for RNase L expression (Fig. 12). RNaseL was detected as a 80k Da band in the testis and spleen; liver showed lower band(s) and prostate showed higher bands in addition to the 80 kDa band. Out of these tissues, the prostate, testis and spleen showed significantly higher expression levels relative to the liver, brain and kidney. Two prominent bands in liver, at about 38kDa were observed which need further characterization. The prostate showed dark signal in the whole lane upto 80kDa band; this may be due to improper extraction or denaturation during the sample preparation. This may also reflect that RNase L may be associated with other proteins in the tissue. Kidney and brain did not show the expression. This also showed differential expression of RNase L in mouse tissues.

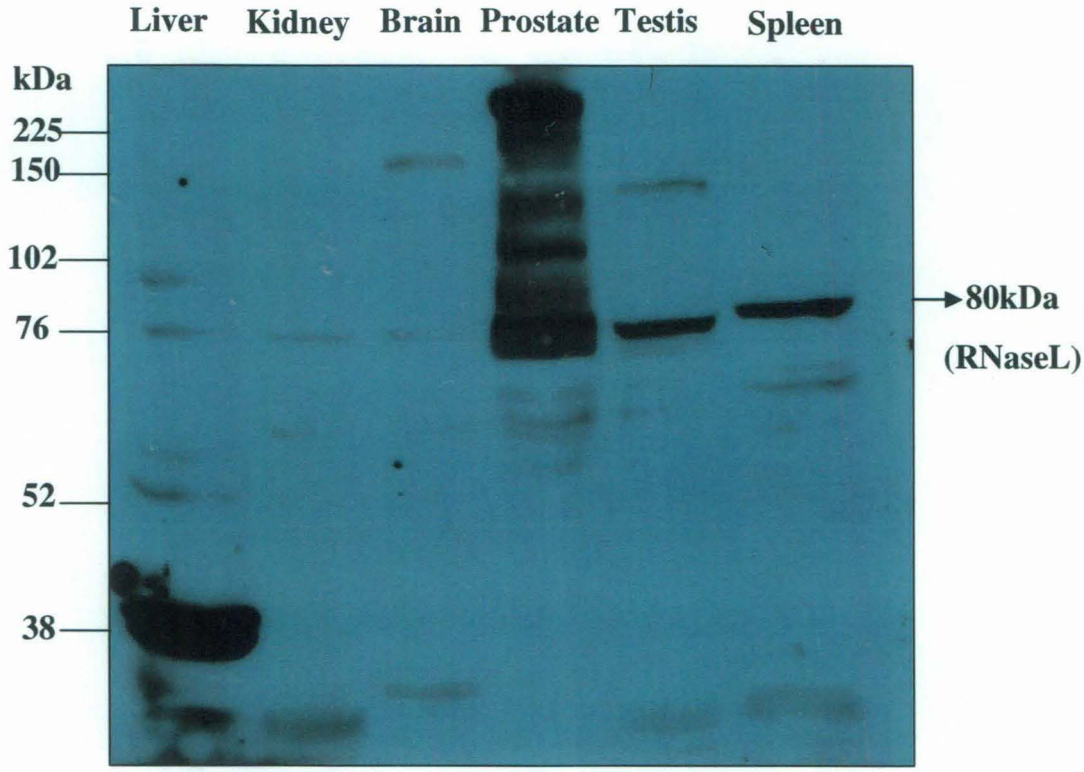

Fig:12 Expression of RNase L protein in the mouse tissues by western blot analysis. 100 µg of tissue extracts from the liver, kidney, brain, prostate, testis and spleen were separated by 8% SDS-PAGE western blotted to n itrocellulosemembrane and immunoblotted with anti-mouse RNase L rabbit polyclonal antiserum (1:1000 dilution) in 2.5% non fat milk and developed with anti rabbit goat IgG-HRP secondary polyclonal antibody (1:10000 dilution) in 2.5% nonfat milk and ECL reagent.

VI. Discussion

The present study describes computational and expression analysis of the interferon-inducible, 2-5A-activated, RNase L. The human RNase L and mouse RNase L were compared with other proteins from genome database. RNase L mRNA and protein expressions were studied in different mouse tissues. The objectives of the study were: to find out evolutionary/biochemical relatives of RNase L, and to find indications/implications of broad range expression, function of RNase L.

VI.1. Computational analysis

VI.1.1. RNase L homologue in *E. coli*

In order to find out the homologue of RNase L in *E. coli* genome, BLAST analysis of the RNase L sequence was carried out, which predicted five significant matches (NP_752376.1, NP_286054.1, NP_414852.1, YP_444030.1 and YP_444030.1). All these five sequences showed homology to ankyrin repeat region of RNase L. The sequence NP_752376.1, NP_286054.1, NP_414852.1 and YP_444030.1 belong to same gene family, *YahD*. While NP_286054.1 is a putative transcriptional factor and NP_414852.1 is a predicted transcriptional regulator. The homology predicts that the N-terminal region of RNase L could have evolved form a transcriptional regulator/factor, which may have retained/lost its function. Presence of RNase L in the nucleus of the mammalian cells (Nilsen et al, 1982; Bayard and Gabrion, 1993) also suggests its role in the nucleus. Evidence of RNase L in translational regulation is known (LeRoy et al, 2005), whereas experimental evidence for a role in transcriptional regulation is lacking. A hypothetical protein (O2ColV186) which showed a significant (E-value 3e-12) homology to human RNase L is a putative virulence region of a ColV plasmid from an avian pathogenic *Escherichia coli* (APEC). The pAPEC-O2-ColV, contributes to the pathogenesis of avian colibacillosis (Skyberg et al, 2006).

VI.1.2.Human RNase L and *E. coli YahD*

YahD of *E. coli* has been previously reported to show homology to RNaseL. It was shown that *YahD* shows homology with 90–259 a.a. region of human RNase L due to ankyrin repeats with conserved GKT motifs (Pandey and Rath, 2004). They suggested that 2-5A may bind to *YahD* due to the presence of GKT motif. Here, this report compares *YahD* protein in the light of new knowledge gained from the crystal structure of RNaseL (Tanaka et al, 2004; Nakanishi et al, 2005). Apart from the conserved GKT motif, the important residues involved in 2-5A binding, i.e., 60W, as GWTPL motif is also conserved in the two sequences. The previous reports of the presence of 2-5A in *E. coli* (Brown and Kerr, 1985; Trujillo et al, 1987) also suggests the 2-5A binding proteins in *E. coli.* Thus *YahD* and RNaseL may be evolutionarily linked through ankyrin repeats and GKT motifs.

VI.1.3. RNase L and *E. coli* RNases

Hunam RNase L was compared to seven known *E. Coli* endoribonucleases. Comparison with *E. coli* endoribonucleases using NCBI tool bl2seq did not yield any significant result. The alignment of individual endoribonuclease sequences to human RNase L sequence using align program of EBI showed that *RNase E* has more similarity (Identity, 9.7%; Similarity, 17.7%) than other endoribonucleases. *RNase E* is required for both efficient RNA turnover and rRNA processing in *E. coli*. The cleavage specifities of RNase L and *RNase E* are similar in that RNase L cleaves mainly after UU or UA sequences (Floyed-Smith et al, 1981) and *RNase E* usually cleaves with in the AUU sequences of (G/A)AUU(A/U) (Mudd and Higgins, 1993). The similar result was observed by Zhou et al (1993). Thus *RNase E* and RNase L are related through RNA metabolism.

VI.1.4. RNase domain of RNase L in bacterial genomes

As no significant similarity to the RNase domain of RNase L was found in *E. coli* genome, we looked for the homologous sequences to RNase

domain (587-741aa) of RNase L in all the completed bacterial genomes. The search did not yield any significant result. Thus, it seems that homology to RNase domain is absent in prokaryotes.

VI.1.5. RNase L homologue in protozoan genomes

Search for homologues of human RNase L in protozoan genomes yielded homologues mainly in the ankyrin repeat region, and a protein having homology to the kinase and RNase domains of RNase L. The ankyrin repeat of RNase L has shown homology in the *E. coli* genome, with almost similar E-values to that of E-values of protozoan homologues to RNase L's ankyrin repeat region. Considering the highly conserved and ubiquitous presence of ankyrin repeats in all genomes of all phyla, the ankyrin region homologues were not considered for further studies.

A protein *IreA* of *Dictyostelium discoideum* (XP_647192.1) showed homology to the protein kinase and RNase domain of RNase L. The dictyostelium *IreA* shows homology to 358-712 aa of human RNase L with an E- value of $3e^{-14}$. It also has the conserved residues important for the RNase activity of RNase L. *Dictyostelium* amoebae inhabit forest soil and consume bacteria and yeast, which they track by chemotaxis. Starvation, however, prompts the solitary cells to aggregate and develop as a true multicellular organism, producing a fruiting body comprised of a cellular, cellulosic stalk supporting a bolus of spores. This is an example of stress-inducible differentiation. Thus, *Dictyostelium* has evolved mechanisms that direct the differentiation of a homogeneous population of cells into distinct cell types, regulate the proportions between cell types and orchestrate the construction of an effective structure for the dispersal of spores. Many of the genes necessary for these processes in *Dictyostelium* were also inherited by Metazoa and fashioned through evolution for use within many different modes of development (Eichinger et al., 2005). Presence of a homologue of RNase L at the interface of unicellularity and multicellularity shows the evolution of RNase domain of RNaseL in relatively complex forms of life rather than its presence in much simpler forms likes bacteria. It remains to be investigated if *IreA* is involved in the cell differentiation program of *Dictyostelium*.

VI.1.6. RNase L homologue in yeast genome

As no program at NCBI was available for homology search with all the sequenced fungal genomes (as in the case of bacterial and protozoan genomes), yeast genome was selected for homology search as it is the one of the well studied fungal genome. The results showed homology to a protein kinase and endoribonuclease, Ire1p, and some ankyrin repeat proteins. Interestingly, the E-values of the homologous proteins to ankyrin repeats are much higher than that of the proteins in the bacterial or protozoan genome. The yeast *Ire1p* was previously reported as a RNase L-homologue (Dong et al, 2001). The *Ire1p* is an endoribonuclease and kinase, which is involved in endoplasmic reticulum stress response (ER-stress) in yeast and mammalian cells and has been linked to restoration of misfolded proteins (Tirasophon et al, 1998). This has also been referred to as unfolded protein response (UPR). Biochemical studies on RNase L and *Ire1p* have shown partially overlapping RNase domain in the two proteins. Two residues, that are essential for the activity of yeast *Ire1p* (H976 and P977) are not required in human RNase L (H583 and P584), while the residues, D661, and H672 are important for the activity in both RNase L and *Ire1p*. The substrate specificities of the two proteins are also mutually exclusive (Dong et al, 2001). Homology of RNaseL and *Ire1p* makes RNase L homology with *IreA* more significant.

VI.1.7. RNase L homologue in algal genome

After looking into the homology searches in the protozoan and yeast genomes, homology search for human RNase L was carried out with the only sequenced green algae, *Ostreococcus lucimarinus* genome. *Ostreococcus lucimarinus* belongs to the *Prasinophyceae*, an early-diverging class within the green plant lineage, and is reported as a globally abundant, single-celled alga thriving in the upper (illuminated) water column of the oceans. The BLAST result showed the algal homologue to the ankyrin repeat region of RNase L and a sequence (XP_001416089.1), which shows homology to the protein kinase as well as RNase domain of RNase L. The sequence alignment of

XP_001416089.1 showed that it has conserved residues of human RNase L (e.g., 661D, 667A, 672H, add 392K) involved in the catalytic function.

The yeast homologue, Ire1p is a well-characterized protein while the *Dictyostelium* and algal homologues are not yet characterized. Both the algal as well as *Dictyostelium* homologues seem to be the part of *Ire*-superfamily. Presence of the homologue in the most "primitive" organism of three major phyla, i.e., Plant (algae), protozoan (*Dictyostelium*) and fungal (yeast) genomes indicates that the *Ire* is a highly conserved protein in all eukaryotes, possibly mediating stress response. Earlier study from our laboratory (Pandey Bajaj and Rath, 2004) has reported that RNase L is also involved in cellular stress response. It is induced by a variety of stressors in human cells and has similarity with *Ire1p*. Although, the homology to RNase L is present in the primitive organisms of three major phyla, i.e., plant (algae), protozoan (*Dictyostelium*) and fungal (yeast); the presence of RNase L only in the higher vertebrates has been reported (Cayley et al., 1982, Bali and white, 1978).

The findings from the studies, that expression of human RNase L in *E. coli* lead to cell growth-inhibition and RNA degradation and the subsequent finding of *YahD* as a homologue of human RNase L (Pandey and Rath, 2004) indicates that the homology to the regulatory region of RNase L might have been originated from *E. coli*, while the sensor domain of *Ire1p* of yeast does not show any significant homology to the regulatory domain of RNase L. This fact suggests that the regulatory domain (ankyrin repeat region) may have a prokaryotic origin. The catalytic domain and the RNA binding domain of RNase L might have originated from the *Ire1p* of the yeast. RNase L is thus a conceptual hybrid of *YahD* and *Ire1p*. This may suggest that evolution of RNase L as an endoribonuclease with ankyrin repeats is a later event than its RNase activity and this some how must have been linked to infection by microorganisms in order to link it to the interferon genes and the innate immune system of the vertebrates, which also should be linked to the 2-5OAS family of genes, in order to link it to the 2-5A cofactor inducibility of RNase L. A possible hypothesis may be by horizontal gene transfer for RNase L gene and gene duplication for 2-5OAS and interferon genes.

VI.1.8. Comparison of RNase L human and mouse RNase L

Comparison of human and mouse RNase L proteins showed that they are highly homologous proteins in all 9 ankyrins, protein kinase, cysteine-rich region and RNase region. Functionally characterized residues are also conserved in both the molecules, except the arginine 462 which is replaced by histidine in mouse.

VI.1.9. Disordered regions in mouse RNase L and human RNase L

In spite of high homology in all the regions of human and mouse RNase L, they showed difference in the predicted disordered regions. The Two parameters were used for disordered prediction (Linding, 2003). (1) Missing coordinates in X-Ray structure as defined by REMARK465 entries in PDB. Non assigned electron densities most often reflect intrinsic disorder, and have been used in disorder prediction. (2) Hot loops definition constitute a refined subset of the above, namely those loops with a high degree of mobility as determined from C-α temperature factors (B-factors). It follows that highly dynamic loops should be considered for protein disorder. The Remarks465 picked four disordered regions in the human RNase L, while only one in the mouse protein. According to this definition, the sequence 1-24 is disordered in both human and mouse RNase L. The hot loop definition showed nine disordered regions in human RNase L sequence and twelve disordered regions in the mouse protein. Out of these twelve disordered regions, seven were conserved in the human protein also. These identified conserved disordered regions could be further analyzed computationally and biochemically to find new functions of the protein.

VI.1.10. Hydropathy Plot

The hydrophobicity pattern shown by human RNase L and mouse RNase L is similar, with some difference in the hydrophobicity of a region in the 4^{th}-ankyrin repeat, which is involved in 2-5A binding. It is known that 2-5A must have at least one (in human) or two (in mice) 5'-phosphoryl groups

and a minimum of three adenylyl residues in 2', 5' linkage to activate RNase L. (Cayley, Davies et al., 1984). The difference in hydrophobicity shown by the hydropathy plots could account for the different specificities of the two molecules for 2-5A.

VI.2. Expression analysis

Expression of RNase L has been studied as early as 1980s by virtue of its property to bind with 2-5A. Using radiolabelled 2-5A, many workers studied expression of RNase L in different tissues and organisms (Williams et al., 1979, Nilsen et al., 1981, Krause and Silverman, 1993). Expression of RNaseL in mouse has been already shown in mouse liver, kidney, lung, intestine, spleen, brain, testis, thymus, intestine and heart using radiolabelled 2-5A. (Nilsen et al, 1981; Floyed-Smith and Denton, 1988; Silverman et al, 1988).

The monoclonal antibody against human RNaseL developed by Silverman's group (Dong and Silverman, 1995) is available commercially but analysis of expression of RNase L using antibody based approach in case of mouse has been rather limited. In 1985, Silverman's group raised polyclonal antibodies against murine RNase L (Dieffenbach et al., 1985). There are no other papers, where this antibody has been used. Later in 1991, Bisbal's group in France (Bisbal et al, 1991) raised polyclonal antibodies against RNaseL, using purified RNaseL from the mouse spleen. They showed western blot of extract from the mouse spleen and cytoplasmic localization of RNase L in NIH 3T3 cells (Bisbal et al, 1991). The use of this antibody is also not found in literature. In 1997, Zhou et al (Zhou et al, 1997) showed western blot of RNase L in the mouse embryonic fibroblasts (MEFs). They expressed the insoluble fragment (99-616 aa) of murine RNase L in the *E. coli* XL-1 blue cells, raised the antibody and removed the non-specific antibodies by incubation with the resuspended pellets of XL-1 blue cells. There are no further reports of use of this antibody also. The mouse monoclonal antibody against human RNase L has been successfully used in many studies and reported in literature.

The present study shows the differential expression of RNase L mRNA and protein in different mouse tissues. The levels of mRNA and protein in the tissues show corresponding levels of expression (except in kidney the RT-PCR result needs confirmation). The presently used anti-mouse RNase L polyclonal antibody can be used for further experiments.

RNase L has been studied during stress conditions like viral infection, chemical stress and in cancer. Investigating role of RNase L in normal tissues may be interesting. A differential expression pattern of RNase L particularly its high expression in immunologically (spleen) and reproductively (testis) important tissues encourages us to look for its role in immunity in normal cells and in reproduction. Further, *in vivo* studies of this unique endoribonuclease in normal as well as abnormal cells and tissues may inform us about its function during normal physiology and pathology.

VII. Conclusions

From the computational and expression analysis of interferon-inducible 2',5'-oligoadenylate (2-5A)-dependent RNase L, it was concluded that –

1. *YahD* of *E. coli* shows highest homology to mammalian RNase L. *YahD* showed homology to the ankyrin repeat region of the RNase L. The nucleotide binding GKT motif and 2-5A binding GWTPL motif is conserved in both human RNase L and *YahD* of *E. coli.*
2. Probably, the RNase domain of RNase L is absent in prokaryotes, as no significant homology to the RNase domain were found in bacterial genomes.
3. *Ire* is the homologue of RNase L which is found in eukaryotes. *IreA* of *Dictyostelium*, *Ire1p* of yeast and and an algal protein (XP_001416089.1) showed homology to the protein kinase region and RNase domain of RNase L, showing evolutionary relationship.
4. Mouse and human RNase L showed high homology of the protein sequences. Mouse and human RNase L sequences showed common disordered sequences while hydropathy plot showed similar hydropathy profile for the two sequences, with difference in the 4^{th} ankyrin repeat suggesting different specificities for 2-5A.
5. RNase L mRNA showed differential expression in the mouse tissues. RNase L protein also showed different sizes and different levels of expression in the mouse tissues suggesting tissue-specific functions of RNase L.

VIII. REFERENCES

Altschul, Stephen F., Thomas L. Madden, Alejandro A. Schäffer, Jinghui Zhang, Zheng Zhang, Webb Miller, and David J. Lipman (1997). Gapped BLAST and PSI-BLAST: a new generation of protein database search programs. *Nucleic Acids Res.* **25**:3389-3402.

Andersen DS, Leevers SJ (2007). The essential Drosophila ABC domain protein, pixie, binds the 40S ribosome in an ATP-dependent manner and is required for translation initiation. *J. Biol. Chem.*, **282:**14752-14760.

Austin A, James C, Silverman RH, Daniel JJ (2005). Critical role for the oligoadenylate synthetase/RNase L pathway in response to IFN-β during acute ocular herpes simplex virus type 1 Infection. *J. Immun.* **175**: 1100–1106.

Baglioni C, Benedetti AD, Williams GJ (1984). Cleavage of nascent reovirus mRNA by localized activation of the 2'-5'-oligoadenylate-dependent endoribonuclease. *J. Virol.* **52**: 865-71.

Bartsch DK, Fendrich V, Slater EP, Sina-Frey M, Rieder H, Greenhalf W, Chaloupka B, Hahn SA, Neoptolemos JP, Kress R (2005). RNASEL germline variants are associated with pancreatic cancer. *Int. J. Cancer* **117**:718-722.

Bayard BA, Gabrion JB (1993). 2',5'-oligoadenylate-dependent RNase located in nuclei: biochemical characterization subcellular distribution of the nuclease in human and murine cells. *Biochem. J.* **296** (Pt 1): 155-160.

Beattie E, Denzler KL, Tartaglia J, Perkus ME, Paoletti E, and Jacobs BL (1995). Reversal of the interferon-sensitive phenotype of a vaccinia virus lacking E3L by expression of the reovirus S4 gene. *J. Virol.* **69**: 499-505.

Bettoun DJ, Scafonas A, Rutledge SJ, Hodor P, Chen O, Gambone C, Voge R, McElwee-Witmer S, Bai C, Freedman L, Schmidt A (2005). Interaction between the androgen receptor and RNase L mediates a cross-talk between the interferon and androgen signaling pathways. *J. Bio. Chem.* **280**: 38898–38901.

Bisbal C, Martinand C, Silhol M, Lebleu B, Salehzada T (1995). Cloning and characterization of a RNAse L inhibitor. A new component of the interferon-regulated 2-5A pathway. *J. Biol. Chem.* **70**: 13308-13317.

Bisbal C, Silhol M, Laubenthal H, Kaluza T, Carnac G, Milligan L, Le Roy F, Salehzada T (2000). The 20-50 oligoadenylate/RNase L/RNase L inhibitor pathway regulates both MyoD mRNA stability and muscle cell differentiation. *Mol. Cell Biol.* **20**: 4959 – 4969.

Bisbal C, Silverman RH, (2007). Diverse functions of RNase L and implications in pathology. *Biochimie* 89:789-798.

Borden EC, Sen GC, Uze G, Silverman RH, Ransohoff RM, Foster GR, Stark GR (2007). Interferons at age 50: past current and future impact on biomedicine. *Nat Rev Drug Discov.* **6**(12):975-90

Bork P, Sander C (1993). A hybrid protein kinase-RNase in an interferon-induced pathway. *FEBS Lett.* **15**:149–152.

Bradford M. M. (1976). A rapid and sensitive method for the quantitation of microgram quantities of protein utilizing the principle of protein dye binding. *Annal. Biochem.* **72**: 248-254.

Breeden L, Nasmyth K (1987). Similarity between cell-cycle genes of budding yeast and fission yeast and the Notch gene of *Drosophila. Nature* **329**: 651–654.

Brown RE and Kerr IM (1985). (p)pp(A2'p)nA is rare in normal mouse tissue and while (A2'p)nA but not (p)pp(A2'p)nA appears to be present in *E. coli Prog. Clin. Biol. Res.* **202**: 3-10

Carpten J, Nupponen N, Isaacs S, Sood R, Robbins C, Xu J, Faruque M, Moses T, Ewing C, Gillanders E, Hu P, Bujnovszky P, Makalowska I, Baffoe-Bonnie A, Faith D, Smith J, Stephan D, Wiley K, Brownstein M, Gildea D, Kelly B, Jenkins R, Hostetter G, Matikainen M, Schleutker J, Klinger K, Connors T, Xiang Y, Wang Z, De Marzo A, Papadopoulos N, Kallioniemi OP, Burk R, Meyers D, Gronberg H, Meltzer P, Silverman R, Bailey-Wilson J, Walsh P, Isaacs W, Trent JM (2002). Germline mutation in ribonuclease L gene in hereditary prostrate cancer 1 (HPC1) linked families. *Nat. Genet.* **30**:181-184.

Casey G, Neville PJ, Plummer SJ, Xiang Y, Krumroy LM, Klein EA, Catalona WJ, Nupponen N, Carpten JD, Trent JM, Silverman RH, Witte JS (2002). RNASEL Arg462Gln variant is implicated in up to 13% of prostate cancer cases. *Nat. Genet.* **32**: 581-583.

Castelli JC, Hassel Katherine BA, Wood A, Li XL, Amemiya K, Dalakas M C, Torrence PF, Youle RJ (1997). A study of the interferon antiviral mechanism: apoptosis activation by the 2-5A system. *J. Exp. Med.* **186**: 967-72.

Cayley PJ, Davies JA, McCullagh KG, Kerr IM (1984). Activation of the ppp(A2'p)nA system in interferon-treated, herpes simplex virus-infected cells and evidence for novel inhibitors of the ppp(A2'p)nA-dependent RNase. *Eur J Biochem* **143**(1): 165-174.

Cayley PJ, White RF, Antoniw JF, Walesby NJ, Kerr IM (1982). Distribution of the ppp(A2'p)nA-binding protein and interferon-related enzymes in animals, plants, and lower organisms. *Biochem Biophys Res Commun.* **108**(3):1243-50

Chandrasekaran K, Mehrabian Z, Li XL, Hassel B (2004). RNase-L regulates the stability of mitochondrial DNA-encoded mRNAs in mouse embryo fibroblasts. *Biochem. Biophys. Res. Comm.* **325**: 18 – 23.

Chebath J, Benech P, Revel M, Vigneron M (1987). Constitutive expression of (2'-5') oligo A synthetase confers resistance to picornavirus infection. *Nature* **330**: 587-8.

Chelbi-Alix MK, Wietzerbin J (2007). Interferon, a growing cytokine family: 50 years of interferon research. *Biochimie* **89**:713-718

Chen Z, Dong J, Ishimura A, Daar I, Hinnebusch AG, Dean M (2006) The Essential Vertebrate ABCE1 Protein Interacts with Eukaryotic Initiation Factors J. Biol. Chem., 281:7452-7457

Defilippi P, Huez G Verhaegen-Lawalle M, De Clercq E, Imai J, Torrence P, Content J. (1986). Antiviral activity of a chemically stabilized 2- 5A analog upon microinjection into HeLa cells. *FEBS Lett.* **198**: 326-32.

Defilippi P, Huez G Verhaegen-Lewalle M, De Clercq E, Torrence P, Content J. 1985). Antiviral activity towards VSV and Mengo virus of a chemically stabilized 2-5A analog upon microinjection into HeLa cells. *Prog. Clin. Biol. Res.* **202**: 141-6.

Demettre E, Bastide L, D'Haese A, Smet KD, Meirleir DK, Tiev KP, Englebienne P, Lebleu B (2002). Ribonuclease L proteolysis in peripheral blood mononuclear cells of chronic fatigue syndrome patients. *J. Biol. Chem.* **277**: 35746-35751.

Diaz-Guerra M, Rivas C, Esteban M (1997). Inducible expression of the 2-5A synthetase/RNase L system results in inhibition of vaccinia virus replication. *Virology* **227**: 220-8.

Diaz-Guerra M, Rivas C, Esteban M (1999). Full activation of RNase L in animal cells requires binding of 2-5A within ankyrin repeats 6 to 9 of this interferon-inducible enzyme. *J. Interferon Cytokine Res* **19**: 113–119.

Dieffenbach CW, Krause D, Silverman RH (1985). Polyclonal antibody directed against 2-5A-dependent RNase. *Prog Clin Biol Res.* **202**:105-14

Dong B and Silverman RH (1995). 2-5A-dependent RNase molecules dimerize during activation by 2-5A. *J Biol Chem* **270**(8): 4133-7.

Dong B and Silverman RH (1997). A bipartite model of 2-5A-dependent RNase L. *J Biol Chem* **272**(35): 22236-42.

Dong B, Kim S, Hong S, Gupta JD, Malathi K, Klein EA, Ganem D, De-Risi J, Chow SA, Silverman RH (2007). An infectious retrovirus susceptible to an interferon antiviral pathway from human prostate tumors. Proc. Natl. Acad. Sci. USA 104: 1655-1660.

Dong B, Niwa M, Walter P, Silverman RH (2001). Basis for regulated RNA cleavage by functional analysis of RNase L and Ire1p. *RNA* **7**: 361-373.

Dong B, Silverman RH (1997). A bipartite model of 2-5A-dependent RNase L. *J. Biol. Chem.* **272**: 22236–22242.

Dong B, Silverman RH (1999). Alternative function of a protein kinase homology domain in 2'- 5'-oligoadenylate dependent RNase L. *Nucleic Acids Res.* **27**:439–445.

Dong B, Xu L, Zhou A, Hassel BA, Lee X, Torrence PF, Silverman RH (1994). Intrinsic molecular activities of the interferon-induced 2-5A-dependent RNase. *J. Biol. Chem.* **269**:14153-8.

Dupuis S, Jouanguy E, Al-Hajjar S, Fieschi C, Al-Mohsen IZ, Al-Jumaah S, Yang K, Chapgier A, Eidenschenk C, Eid P, Al Ghonaium A, Tufenkeji H, Frayha H, Al-Gazlan S, Al-Rayes H, Schreiber RD, Gresser I, Casanova JL (2003). Impaired response to interferon-alpha/beta and lethal viral disease in human STAT1 deficiency. *Nat. Genet.* **33**: 388–391.

Eichinger L, Pachebat J A, Glöckner G, Rajandream MA, Sucgang R, Berriman M et al (2005). The genome of the social amoeba *Dictyostelium discoideum. Nature* **435**, 43-57.

Floyd-Smith G, Slattery E, Lengyel P (1981). Interferon action: RNA cleavage pattern of a 2'-5'oligoadenylate dependent ribonuclease. *Science* **212**: 1020-1032.

Floyed-Smith G, Denton JS (1988). A (2'-5')An-dependent endonuclease: tissue distribution in BALB/c mice and the effects IFN-beta treatment and anti-IFN-alpha/beta immunoglobulin on the levels of the enzyme. *J. Interferon Res.* **8**: 517-525.

Fremont M, Bakkouri KE, Vaeyens F, Herst CV, Meirleir KD, Englebienne P (2005). 2',5'-Oligoadenylate size is critical to protect RNase L against proteolytic cleavage in chronic fatigue syndrome. *Exp. Mol. Pathol.* **78**:239-246.

Gabaldon T, Huynen MA (2004). Prediction of protein function and pathways in the genome era. *Cell Mol. Life Sci.* **61**: 930-944.

Gresser I, Bourali C, Levy JP, Fontaine-Brouty-Boye D, Thomas MT (1969), Increased survival in mice inoculated with tumor cells and treated with interferon preparations. *Proc. Natl. Acad. Sci. U.S.A.* **63** 51-57.

Hall, TA (1999). BioEdit: a user-friendly biological sequence alignment editor and analysis program for Windows 95/98/NT. *Nucl. Acids. Symp. Ser.* **41**:95-98.

Hassel BA, Zhou A, Sotomayor C, Maran A, Silverman RH (1993). A dominant negative mutant of 2-5Adependent RNase suppresses antiproliferative and antiviral effects of interferon. *EMBO J.* **12**: 3297 – 3304.

Hearl WG and Johnston MI (1987) Accumulation of 2',5'-oligoadenylates in encephalomyocarditis virus-infected mice. *J Virol.* **61**(5): 1586-1592

Hovanessian AG, Wood J, Meurs E, LucOntagnier (1979). Increased nuclease activity in cells treated with pppA2'p5'A2'p5'A. *Proc. Natl. Acad. Sci. USA* **76**: 3261-3265.

Hovanessian AG, Wood JN, Meurs E, Montagnier L (1980). Anticellular and antiviral effects of pppA(2'p5'A)n. *Virology* **101**: 81 – 90.

Ikeda, H., Old, L.J., and Schreiber, R.D. (2002). The roles of IFN gamma in protection against tumor development and cancer immunoediting. *Cytokine Growth Factor Rev* **13:** 95–109.

Isaacs A, Lindenmann J (1957), Virus interference. I. The interferon. *Proc. R. Soc. Lond. B.* **147**: 258-267.

Jacobs MD, Harrison SC (1998) Structure of an IkBa/NF-kB complex. *Cell* **95**: 749–758.

Jacobsen H, Krause D, Friedman RM, Silverman RH (1983). Induction of ppp(A2'p)nA- dependent RNase in murine JLSV9R cells during growth inhibition. *Proc. Natl. Acad. Sci. USA* **80**:4954 – 4958.

Kalinichenko EN, Podkopaeva TL, Budko EV, Seela F, Dong B, Silverman RH, Vepsalainen J, Torrence PF and Mikhailopuloa IA (2004). 3-Deazaadenosine analogues of p5'A2'p5'A2'p5'A: synthesis, stereochemistry, and the roles of adenine ring nitrogen-3 in the interaction with RNase L *Bioorg Med Chem.* **12**: 3637–3647

Kerr ID (2004). Sequence analysis of twin ATP binding cassette proteins involved in translational control, antibiotic resistance, and ribonuclease L inhibition. *Biochem. Biophys. Res. Comm.* **315**: 166-173.

Kerr IM, Brown RE (1978). pppA2'p5'p2'p5'A: an inhibitor of protein synthesis synthesized with an enzyme fraction from interferon treated cells. *Proc. Natl. Acad. Sci. USA* **75**: 256-260.

Khabar KS, Siddiqui YM, Al-Zoghaibi F, Al-Haj L, Dhalla M, Zhou A, Dong B, Whitmore M, Paranjape J, Al-Ahdal M, Al-Mohanna F, Williams BR, Silverman RH (2003). RNase L mediates transient control of interferon response through modulation of the double-stranded RNA dependent protein kinase PKR. *J. Biol. Chem.* **278**: 20124 – 20132.

Kispal G, Sipos K, Lange H, Fekete Z, Bedekovics T, Janáky T, Bassler J, Netz DJA, Balk J, Rotte C, Lill R (2005). Biogenesis of cytosolic ribosomes requires the essential iron–sulphur protein Rli1p and mitochondria. *EMBO J.* **24**: 589–598.

Krause D, Lesiak K, Imai J, Sawai H, Torrence PF, and Silverman RH (1986). Activation of 2-5A-dependent RNAse by analogues of 2-5A (5'-O-triphosphoryladenylyl(2'----5')adenylyl(2'----5')adenosine) using 2',5'-tetraadenylate (core) cellulose. *J. Biol. Chem.* **261**: 6836-6839.

Krause D, Mullins JM, Penafiel LM, Meister R, Nardone RM (1991). Microwave exposure alters the expression of 2-5A-dependent RNase. *Radiat Res.* **127**:164-70.

Krause D, Panet A, Arad G, Dieffenbach CW, and Silverman RH (1985) Independent regulation of ppp(A20p)nA dependent RNase in NIH 3T3, clone 1 cells by growth arrest and interferon treatment. *J. Biol. Chem.* **260**: 9501 – 9507.

Krause D, Silverman RH (1993). Tissue-related and species-specific differences in the 2-5A oligomer size requirement activation of 2-5A-dependent RNase. *J. Interferon Res.* **132**: 13-16.

Kruger S, Silber AS, Engel C, Gorgens H, Mangold E, Pagenstecher C, Holinski-Feder E, Doeberitz MK, Moeslein G, Dietmaier W, Stemmler S, Friedl W, Ruschoff J, Schackert HK (2005). Arg462Gln sequence variation in the prostate- cancersusceptibility gene RNASEL and age of onset of hereditary non-polyposis colorectal cancer: a case-control study. *Lancet Oncol.* **6**: 566-572.

Laemmli UK, (1970). Cleavage of structural proteins during the assembly of the head of bacteriophage T4. *Nature* **229** (259):680-685.

LeRoy F, Bisbal C, Silhol M, Martinand C, Lebleu B, Salehzada T (2001). The 2-5A/RNase L/RNase L inhibitor (RLI) [correction of (RNI)] pathway regulates mitochondrial mRNAs stability in interferon alpha-treated H9 cells. *J. Biol.Chem.* **276**: 48473 – 48482.

LeRoy F, Laskowska A, Silhol M, Salehzada T, Bisbal C (2000). Characterization of RNABP, an RNA binding protein that associates with RNase L. *J. Interferon Cytokine Res.* **20**: 635-644.

LeRoy F, Salehzada T, Bisbal C, Dougherty JP, Peltz SW (2005). A newly discovered function for RNase L in regulating translation termination. *Nat. Struct. Mol. Biol.* **12**: 505-512.

Li G, Xiang Y, Sabapathy K, Silverman RH (2004). An apoptotic signaling pathway in the interferon antiviral response mediated by RNase L and c-Jun NH_2-terminal kinase. *J. Biol. Chem.* **279**:1123–31.

Li XL, Blackford JA, Hassel BA (1998). RNase L Mediates the Antiviral Effect of interferon through a selective reduction in viral RNA during encephalomyocarditis virus infection. *J. Virol.* **72**: 2752-2759.

Li XL, Blackford JA, Judge CS, Liu M, Xiao W, Kalvakolanu DV, Hassel BA (2000). RNase-L-dependent destabilization of interferon-induced

mRNAs. A role for the 2-5A system in attenuation of the interferon response. *J. Biol. Chem.* **275**: 8880 – 8888.

Linding R, Jensen LJ, Diella F, Bork P, Gibson TJ, Russell RB (2003) Protein disorder prediction: implications for structural proteomics. *Structure* **11**:1453-1459

Liu W, Liang SL, Liu H, Silverman R, Zhou A. (2007) Tumour suppressor function of RNase L in a mouse model. *Eur. J. Cancer* **43**: 202 –209.

Lux SE, John, KM, Bennett V (1990). Analysis of cDNA for human erythrocyte ankyrin indicates a repeated structure with homology to tissue-differentiation and cell-cycle control proteins. *Nature* **344**: 36–42.

Malathi K, Dong B, Jr MG, Silverman RH (2007). Small self-RNA generated by RNase L amplifies antiviral innate immunity. *Nature* **448**:| doi:10.1038/nature06042.

Malathi K, Paranjape JM, Ganapathi R, Silverman RH (2004). *HPC1/RNASEL* mediates apoptosis of prostate cancer cells treated with 2',5'-oligoadenylates, topoisomerase I inhibitors, and tumor necrosis factor-related apoptosis-inducing ligand. *Cancer Res.* **64**: 9144–9151.

Marcotte EM, Pellegrini M, Yeates TO, Eisenberg, D (1999). A census of protein repeats. *J. Mol. Biol.* **293**: 151–160.

Mudd EA, Higgins CF (1993). *Escherichia coli* endoribonuclease RNase E: autoregulation of expression and site-specific cleavage of mRNA *Mol Microbiol* **9** (3), 557–568.

Naito T, Yokogawa T, Kim HS, Matsuda A, Sasaki T, Fukushima M, Kitade Y, Wataya Y (2006). An apoptotic pathway of 3'-Ethynylcytidine (ECyd) involving the inhibition of RNA synthesis mediated by RNase L. *Nucleic Acids Symposium Series* **50**:103-104.

Nakanishi M, Tanaka N, Mizutani Y, Mochizuki M, Ueno Y, Nakamura KT, Kitade Y (2005). Functional characterization of 2',5'-linked oligoadenylate binding determinant of human RNase L. *J Biol. Chem.* **280**: 41694–41699.

Nakanishi M, Yoshimura A, Norihisa Ishida N, Ueno Y, and Kitade Y (2004). Contribution of Tyr712 and Phe716 to the activity of human RNase L. *Eur. J. Biochem.* **271**:2737–2744.

Nilsen TW, Wood DL, Baglioni C (1981). 2',5'-Oligo(A)-activated endoribonuclease: Tissue distribution and characterization with a binding assay. *J. Biol. Chem.* **256**: 10751-10754.

Nilsen TW, Wood DL, Baglioni C (1982). Presence of 2'-5'-oligo(A) and of enzymes that synthesize, bind, and degrade 2'-5'-oligo(A) in HeLa cell nuclei. *J. Biol. Chem.* **257** (4): 1602-1605.

Palenik B, Grimwood J, Aerts A, Rouze P, Salamov A, Putnam N, Dupont C, Jorgensen R, Derelle E, Rombauts S, Zhou K, Otillar R, Merchant SS, Podell S, Gaasterland T, Napoli C, Gendler K, Manuell A, Tai V, Vallon O, Piganeau G, Jancek S, Heijde M, Jabbari K, Bowler C, Lohr M, Robbens S, Werner G, Dubchak I, Pazour GJ, Ren Q, Paulsen I, Delwiche C, Schmutz J, Rokhsar D, Van de Peer Y, Moreau H, Grigoriev IV (2007). The tiny eukaryote Ostreococcus provides genomic insights into the paradox of plankton speciation. *Proc Natl Acad Sci USA* 104 (18): 7705-7710

Pandey M, Bajaj GD, Rath PC (2004) Induction of the Interferon-Inducible RNA-Degrading Enzyme, RNase L, BY Stress Inducing Agents in the Human Cervical Carcinoma Cells. *RNA Biol,* 1:1, 21-27.

Pandey M, Rath PC (2004). Expression of interferon-inducible recombinant human RNase L causes RNA degradation and inhibition of cell growth in *E.coli. Biochem. Biophys.l Res. Comm.* **317**: 586–597.

Paucker K, Cantell K, Henle W (1962). Quantitative studies on viral interference in suspended L cells. III. Effect of interfering viruses and interferon on the growth rate of cells. *Virology* **17**: 324-334.

Pearson W.R. and Lipman D.J. (1988) Improved Tools for Biological Sequence Comparison. *Proc Natl Acad Sci USA* **85**: 2444-2448.

Pestka, S., Krause, C.D., and Walter, M.R. (2004). Interferons, interferon-like cytokines, and their receptors. *Immunol Rev* **202**: 8–32.

Rivas C, Gil J, Melkova Z, Esteban M, Diaz-Guerra M. (1998). Vaccinia virus E3L protein is an inhibitor of the interferon (IFN)-induced 2-5A synthetase enzyme. *Virology* **243**: 406-14.

Rusch L, Zhou A, Silverman RH (2000). Caspase-dependent apoptosis by 2',5'- oligoadenylate activation of RNase L is enhanced by IFN-beta. *J. Interferon Cytokine Res.* **20**: 1091-100.

Rysiecki G, Gewert DR Williams BR (1989). Constitutive expression of a 2',5'-oligoadenylate synthetase cDNA results in increased antiviral activity and growth suppression. J Interferon Res. **9**:649-57

Salehzada T, Silhol M, Lebleu B, Bisbal C (1991) Polyclonal Antibodies against RNase L. *J Biol Chem* **266**: 5808-5813,

Samuel CE (2001). Antiviral actions of interferons. *Clin. Microbiol. Rev.* **14**, 778–809.

Samuel MA, Whitby K, Keller BC, Marri A, Barchet W, Williams BRG, Silverman RH, Gale M, Diamond MS (2006). PKR and RNase L contribute to protection against lethal West Nile virus infection by controlling early viral spread in the periphery and replication in neurons. *J.Virol.* **80**: 7009–7019.

Saraste M, Sibbald P R, and Wittinghofer A (1990). The P-loop – a common motif in ATP and GTP-binding proteins. *Trends Biochem. Sci.* **15**: 430-434.

Scherbik SV, Paranjape JM, Stockman BM, Silverman RH, Brinton MA, (2006). RNase L plays a role in the antiviral response to West Nile virus. *J Virology* **80:** *2987–2999.*

Schroder HC, Suhadolnik RJ, Pfleiderer W, Charubala R, Muller WE (1992). (2'-5')Oligoadenylate and intracellular immunity against retrovirus infection. *Int. J. Biochem.* **24**: 55-63.

Sedwick SG, Smerdon SJ (1999). The ankyrin repeat: a diversity of interactions on a common structural framework. *Trends Biochem. Sci.* **24**: 311–316.

Sidrauski C, Walter P (1997). The transmembrane kinase Ire1p is a site-specific endonuclease that initiates mRNA splicing in the unfolded protein response. *Cell* **90**:1031–1039.

Silverman R H (2003). Implications for RNase L in prostate cancer biology. *Biochemistry* **4**: 1805-12.

Silverman RH, Jung DD, Nancy L, Nolan-Sorden, Dieffenbach CW, Kedar VP, and SenGupta DN (1988). Purification and Analysis of Murine 2-5A-dependent RNase. J. Biol. Chem **263**(15):7336-7341.

Silverman RH. Dieffenbach CW, Krause D (1986). 2-5A-dependent RNase is induced during differentiation of embryonal carcinoma (PC13) cells but

not of neuroblastoma (NIE 115) cells. In "Interferons as cell growth inhibitors and antitumor factors" (Friedman RM, Merigan T, Sreevalsan T, eds), pp-143-150. Alan R Liss, New York.

Skyberg JA, Johnson TJ, Johnson JR, Clabots C, Logue CM, Nolan LK (2006). Acquisition of avian pathogenic Escherichia coli plasmids by a commensal E. coli isolate enhances its abilities to kill chicken embryos, grow in human urine, and colonize the murine kidney. *Infect Immun.* **74**(11):6287-92

Suhadolnik RJ, Peterson DL, O'Brien K, Cheney PR, Herst CV, Reichenbach NL, Kon N, Horvath SE, Iacono KT, Adelson ME, De MK, De BP, Charubala R, Pfleiderer W (1997). Biochemical evidence for a novel low molecular weight 2-5A-dependent RNase L in chronic fatigue syndrome. *J. Interferon Cytokine Res.* **17**: 377-385.

Takaoka A and Yanai H (2006). Interferon signalling network in innate defence. *Cell Microbiol.* **8**(6):907–922

Tanaka N, Nakanishi M, Kusakabe Y, Goto Y, Kitade Y ,Nakamura KT (2004). Structural basis for recognition of 2'-5'-linked oligoadenylates by human ribonuclease L. *EMBO J.* **23**(20):3929-38

Tatiana A. Tatusova, Thomas L. Madden (1999), "Blast 2 sequences - a new tool for comparing protein and nucleotide sequences", *FEMS Microbiol Lett.* **174**:247-250

Tirasophon W, Welihinda AA, Kaufman RJ (1998). A stress response pathway from the endoplasmic reticulum to the nucleus requires a novel bifunctional protein kinase/endoribonuclease (Ire1p) in mammalian cells. *Genes & Dev.* **12**: 1812-1824

Trujillo MA, Roux D, Fueri JP, Samuel D, Cailla HL, Rickenberg HV (1987). The occurrence of 2'-5' oligoadenylates in *E. coli. Eur. J. Biochem.* 169, 167-173

Urisman A, Molinaro RJ, Fischer N, Plummer SJ, Casey G, Klein EA, Malathi K, Magi-Galluzzi C, Tubbs RR, Ganem D, Silverman RH, De-Risi JL (2006). Identification of a novel gammaretrovirus in prostate tumors of patients homozygous for R462Q RNASEL variant. *PLoS Pathog.* **2**(3):e25.

Vilcek J (2003). Novel interferons. *Nat Immunol* **4:** 8–9.

Wang L, Zhou A, Vasavada S, Dong B, Nie H, Church JM, Williams BRG, Banerjee S, Silverman RH (1995). Eevated levels of 2',5'-linked oligoadenylate-dependent ribonuclease L occur as an early event in colorectal tmorigenesis. *Clin. Cancer Res.* **1**: 1421-1428.

Wreschner DH, James TC, Silverman RH, Kerr IM (1981). Ribosomal RNA cleavage, nuclease activation and 2-5A(ppp(A2'p)nA) in interferon-treated cells. *Nucleic Acids Res.* **9**:1571-1581.

Wreschner DH, McCauley JW, Skehel JJ, Kerr IM (1981). Interferon action - sequence specificity of the ppp(A2'p)nA-dependent ribonuclease. *Nature* **289**:414-7.

Wreschner DH, Silverman RH, James TC, Gilbert CS, Kerr IM (1982) Affinity labeling and characterization of $(ppp(A2'p)_n$ A dependent endoribonuclease from different mammalian tissues. *Eur. J. Biochem.* **124**: 261-268.

Xiang Y, Wang Z, Murakami J, Plummer S, Klein EA, Carpten JD, Trent JM, Isaacs WB, Casey G, Silverman RH (2003). Effects of RNase L mutations associated with prostate cancer on apoptosis induced by 2',5'-oligoadenylates. *Cancer Res.* **63**: 6795-6801.

Zhou A, Hassel BA, Silverman RH (1993). Expression cloning of 2- 5A-dependent RNAase: a uniquely regulated mediator of interferon action. *Cell* **72**: 753–765.

Zhou A, Malinaro RJ, Malathi K, Silverman RH (2005). Mapping of the human RNASEL promoter and expression in cancer and normal cells. *J. Interferon Cytokine Res.* **25**:595-603.

Zhou A, Paranjape J, Brown TL, Nie H, Naik S, Dong B, Chang A, Trapp B, Fairchild R, Colmenares C, Silverman RH (1997). Interferon action and apoptosis are defective in mice devoid of 2',5'-oligoadenylate-dependent RNase L. *EMBO J.* **16**:6355 – 6363.

Zhou A., Paranjape J (1997). Interferon action and apoptosis are defective in mice devoid of 2',5'-oligoadenylate-dependent RNase L. *EMBL J.* **16**: 6355-63.